frontiers in Earth Science

ORIGINAL RESEARCH
published: 06 August 2021
doi: 10.3389/feart.2021.710758

Late Mesozoic Intracontinental Deformation in the Northern Margin of the North China Craton: A Case Study From the Shangyi Basin, Northwestern Hebei Province, China

Qian Yang[1,2,3], *Wei Shi*[1,3]*, *Guiting Hou*[2]*, *Yu Zhang*[1] and *Yilin Zhao*[1,2,3]

[1]*Institute of Geomechanics, Chinese Academy of Geological Sciences, Beijing, China,* [2]*School of Earth and Space Sciences, Peking University, Beijing, China,* [3]*Key Laboratory of Neotectonic Movement and Geohazard, Ministry of Natural Resources, Beijing, China*

During the late Mesozoic, the East Asian continent underwent a complex tectonic history due to multiple episodes of plate convergence. How the crust responds to the multiple plate convergence in the North China Craton (NCC) remains unclear. Here we undertook field geological investigations and fault-slip vectors analysis of the Shangyi Basin in the western Yanshan fold and thrust belt, northern margin of the NCC. Combined with new geochronological data, we delineate three phases of intracontinental deformation in the area: *1*) NW-SE compression during the Late Jurassic to earliest Cretaceous (ca. 151–141 Ma); *2*) NW-SE extension during the middle–late Early Cretaceous (ca. 135–110 Ma); and *3*) NE-SW compressional deformation later than 110 Ma. The early NW-SE compression controlled the present bulk architecture of the basin, and the subsequent two tectonic events only caused limited reworking of the previous structures. Through balanced cross-section restoration, we estimate the horizontal shortening ratio of the crust in the study area is over 27% due to the NW-SE compression. Moreover, the contribution of tectonic shortening from the north side of the basin is greater than that from the south side. NW-SE compressional deformation is consistent in time with the episode B of the Yanshanian movement (Yanshanian B), which may be influenced by the subduction of the Paleo-Pacific plate beneath East Asia and the closure of the Mongol-Okhosk Ocean. Subsequent NW–SE extension is likely to be associated with the destruction of the NCC during the Early Cretaceous. Extension may result from the roll-back of the Paleo-Pacific plate and post-orogenic collapse of the Mongol-Okhotsk belt. The last NE-SW compressional event may be linked to the remote effect of the final collision between the Qiangtang and Lhasa terranes.

Keywords: north China craton (NCC), Shangyi basin, late mesozoic, intracontinental deformation, yanshanian movement, paleo-Pacific plate subduction

OPEN ACCESS

Edited by:
Xiubin Lin,
Zhejiang University, China

Reviewed by:
Chenyue Liang,
Jilin University, China
Gianluca Vignaroli,
University of Bologna, Italy
Jien Zhang,
Chinese Academy of Sciences (CAS), China
Shaofeng Liu,
China University of Geosciences, China

***Correspondence:**
Wei Shi
shiweinmg@163.com
Guiting Hou
gthou@pku.edu.cn

Specialty section:
This article was submitted to Structural Geology and Tectonics, a section of the journal Frontiers in Earth Science

Received: *17 May 2021*
Accepted: *26 July 2021*
Published: *06 August 2021*

Citation:
Yang Q, Shi W, Hou G, Zhang Y and Zhao Y (2021) Late Mesozoic Intracontinental Deformation in the Northern Margin of the North China Craton: A Case Study From the Shangyi Basin, Northwestern Hebei Province, China. Front. Earth Sci. 9:710758. doi: 10.3389/feart.2021.710758

INTRODUCTION

The North China Craton (NCC), located in the interior of the East Asian continent, has experienced a multi-phase intracontinental deformation since the Mesozoic (Liu, 1998; Liu and Yang, 2000; Zheng et al., 2000; Davis et al., 2001; Cui and Wu, 2002; Cope et al., 2007; Zhang et al., 2007; Li et al., 2012; Liu et al., 2013, 2018; Huang et al., 2015; Li et al., 2016; Y. Wang et al., 2018; Y. C. Wang et al., 2018; Yang and Dong, 2018; Clinkscales and Kapp, 2019; Meng et al., 2019; S. F. Liu et al., 2021). These deformations might be related with the convergence of several independent plates or blocks at the same time, including the Siberian Plate to the north, the Paleo-Pacific Plate to the southeast, and the Qiangtang–Lhasa block to the southwest (**Figure 1A**) (Dong et al., 2007, 2015, 2018; Shi et al., 2015). The Yanshanian intracontinental orogeny (Zheng et al., 2000; Davis et al., 2001; Cope et al., 2007; Zhang et al., 2007; Lin et al., 2013; Huang, 2019) and the subsequent large-scale lithospheric extension and thinning of the NCC (Meng, 2003; Zhu et al., 2011; Zhu and Xu, 2019; Wang et al., 2011, 2012; Lin and Wei, 2018; Liu et al., 2020) are the most representative during the complex Mesozoic tectonic evolution, attracting extensive attention from a large amount of geologists. Multiple research approaches, such as analysis of structural geometry and kinematics (Zhang et al., 2011; Li et al., 2016; Clinkscales and Kapp, 2019), study of palaeo-stress field based on fault-slip data (Zhang et al., 2003; Huang et al., 2015; Yang and Dong, 2018; B. Zhang et al., 2020), study on basin-mountain coupling (Liu and Yang, 2000; Cope et al., 2007; Liu et al., 2007, 2018; Y. C. Wang et al., 2018; Lin et al., 2019; Y. Zhang et al., 2020), geochronology (Wu et al., 2005; Wang et al., 2012, 2015), lithogeochemistry (Dai et al., 2016; Li and Wang, 2018), geophysics (Zheng et al., 2009; Zhu et al., 2011; Zhu and Xu, 2019) and numerical simulation analysis (Hou et al., 2010; Liu et al., 2017; Li and Hou, 2018), have been applied to try to reconstruct the history of intracontinental evolution of the NCC during the late Mesozoic. However, detailed structural analysis of key areas remains inadequate. The timing of the late Mesozoic tectonic regime transition within the NCC was defined on late Middle Jurassic (160 ± 5 Ma) (Zhao et al., 2004), the Late Jurassic-Early Cretaceous (ca. 150–140 Ma) (Zhai et al., 2004) and the Early Cretaceous (ca. 136 Ma) (Niu et al., 2003). Besides, the related geodynamic mechanisms was attributed to the subduction of the Paleo-Pacific plate (Ren et al., 2002; Zhu et al., 2011; Zhu et al., 2018; Zhu and Xu, 2019), a combined effect from the Paleo-Pacific subducting plate and the closure of the Mongol-Okhosk Ocean (Meng, 2003; Wang et al., 2011), and a multi-plate convergence around East Asia (Dong et al., 2015, 2018).

In general, the tectonic evolution of the basins records the process of the regional stress propagation and transition (Shi et al., 2006, 2013, 2020; Li and Hou, 2018; B. Zhang et al., 2020; S. F. Liu et al., 2021). Abundant late Mesozoic intracontinental basins were developed along the northern margin of the NCC (He et al., 1998; Liu et al., 2004; J. Liu et al., 2015; Xu et al., 2016; Lin et al., 2019) and were considered as natural laboratories for studying on intracontinental deformation. In this paper, a multidisciplinary survey has been conducted in the Shangyi Basin, which is a typical area in the northern edge of the NCC that recorded late Mesozoic polyphase deformation events. A multi-technique approach, including field structural measurement, stress inversion of fault-slip vectors, cross-section restoration and balancing, and analysis of zircon U-Pb geochronology, has been performed with the aim to reconstruct the tectonic evolution history of the Shangyi Basin. The new results lead us to delineate at least three-phase of tectonic deformation for the study area during the Late Jurassic to Cretaceous. NW-SE compression in the Late Jurassic-Early Cretaceous controlled the basic tectonic framework of the basin. Furthermore, combined with previous studies, we also discussed the relationship between the paleostress regimes of the Shangyi Basin and different plate tectonic configurations and varying driving forces.

GEOLOGICAL SETTING

The Sino-Mongolian block formed due to the final closure of the Paleo-Asian Ocean along the Solonker–Linxi Suture during the late Paleozoic to early Mesozoic (Davis et al., 2001; Xiao et al., 2003; Eizenhöfer et al., 2014; Li et al., 2015). Meanwhile, the South China block in the south was also final collided with the NCC (Liu et al., 2005; Dong et al., 2011; S. F. Liu et al., 2015; Zhang et al., 2019). These large-scale tectonic events marked the beginning of intracontinental deformation of the NCC. During the late Mesozoic, located between the Sino-Mongolian block and the Siberian plate, the Mongol-Okhotsk Ocean began to close from west to east in a scissor-like fashion (Zorin, 1999; Metelkin et al., 2010). In the meantime, the NCC experienced a remarkable intracontinental orogeny, which is generally referred to as the Yanshan Movement (Dong et al., 2015, 2018; Y. Wang et al., 2018; S. F. Liu et al., 2021). The term Yanshan Movement, which was named by Wong (1927) and was initially employed to describe to Late Jurassic–Early Cretaceous unconformities, magmatism, and mineralization in the Yanshan area, is currently used to define a period of significant tectonism that affected East Asia continent during the late Mesozoic (Zhao et al., 2004; Dong et al., 2015, 2018; Y. Wang et al., 2018). The Yinshan–Yanshan fold and thrust belt in the northern margin of the NCC, which extend west–east from the western Inner Mongolia to western Liaoning province along over 1000 km (Zheng et al., 2000; Davis et al., 2001; Cope et al., 2007; Zhang et al., 2007; Lin et al., 2013), has been known as the most representative product of this intracontinental tectonic event. The Yanshan Movement can usually be divided into three sub-stages. The early stage (Yanshanian A) is marked by the disconformities at the base of the Tiaojishan Formation (Late Jurassic) and expressed by some gentle folds and local thrusts (Hao et al., 2021). The intermediate stage is characterized by the Tiaojishan Formation volcanic rocks (Zhao et al., 2004). And the last stage (Yanshanian B) is represented by a regional unconformity at the base of the Zhangjiakou Formation volcanic rocks (Early Cretaceous) and involved diffuse folding and thrust faulting (Y. Wang et al., 2018; Lin et al., 2019). Following the Yanshan Movement, the northern NCC has

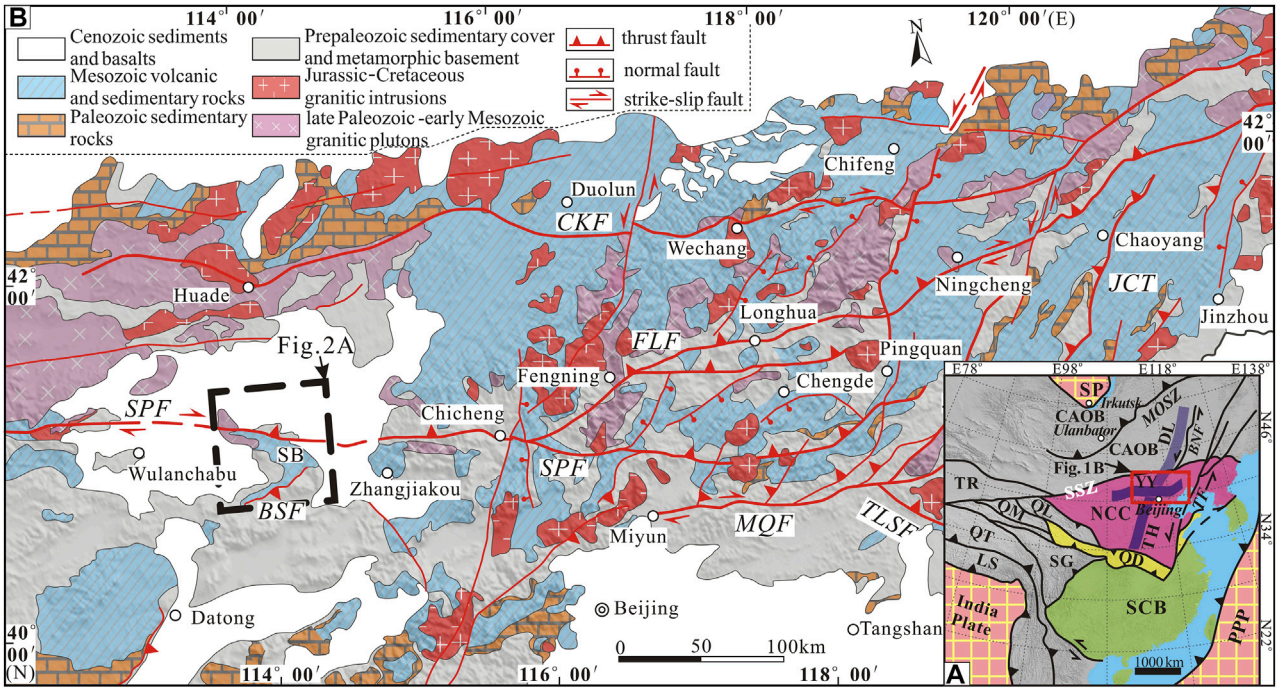

FIGURE 1 | (A) Structural outline of the North China Craton and the surrounding. **(B)** Geological sketch of the northern margin of the North China Carton (modified after Zhang et al., 2006; Zhang et al., 2011). SP, Siberian plate; PPP, Paleo-Pacific plate; IP, Indian plate; NCC, North China Craton; SCB, South China block; QM, Qaidam block; TR, Tarim block; QT, Qiangtang terrane; LS, Lhasa terrane; SG, Songpan-Ganzi belt; CAOB, Central Asian Orogenic Belt; MOSZ, Mongol-Okhotsk suture zone; SSZ, Solonker-Linxi suture zone; YY, Yinshan-Yanshan fold-thrust belt; QD, Qinling-Dabie Orogen; QL, Qinlian belt; TH, Taihang Mountains; DL, Dahingganling; TF, Tan-Lu Fault Zone; BNF, Balihan-Nenjiang Fault Zone; CKF, Chifeng-Kaiyuan Fault; FLF, Fengling-Longhua Fault; JCT, Jianchang-Chaoyang Thrust Fault; SPF, Shangyi-Pingquan Fault; MQF, Miyun-Qinglong Fault; TLSF, Taiying-Lengkou-Shangying Fault; BSF, Banshen-Shuiquangou Fault; SB, Shangyi Basin.

experienced widespread extension and thinning of the continental lithosphere during the Early Cretaceous, expressed by remarkable magmatism (Wu et al., 2011; S. H. Zhang et al., 2014; Wang et al., 2015), graben and half-graben basins (Zorin, 1999; Graham et al., 2001; Ren et al., 2002; Meng, 2003; Liu et al., 2004; Y. Q. Zhang et al., 2004; Li and Hou, 2018; B. Zhang et al., 2020) and low-angle detachment systems or metamorphic core complexes (MCCs) (Liu et al., 2008, 2021; Wang et al., 2011, 2012; Lin and Wei, 2018). Furthermore, a short phase of compression occurred after the late Early Cretaceous, which resulted in an extensive tectonic reverse of the Early Cretaceous faulted basin in Eastern China and adjacent areas (Y. Q. Zhang et al., 2004; B. Zhang et al., 2020). Some works consider this compressional event as the episode C of the Yanshanian Movement, which indicates termination of the NCC peak destruction (Zhang et al., 2008; Zhu et al., 2012).

The Shangyi Basin in the northwest of Hebei province, China, is situated on the intersection area between the ~E-W-trending Yinshan–Yanshan fold and thrust belt and NNE-trending Dahingganling (or Greater Khingan Range) –Taihang Mountain structural belt (**Figure 1B**). The basin, about 800 km^2 in area, is bounded by the ~E-W-striking Shangyi-Pingquan Fault (SPF) to the north and the NE-to NNE-striking Banshen-Shuiquangou Fault (BSF) to the south, respectively (**Figures 1B**, **2A**). The SPF, as the tectonic boundary between the Yanshan fold and thrust belt and the Inner Mongolia Palaeo-uplift, has a long evolutionary history and was marked by significant thrust and dextral strike-slip movement in the late Mesozoic (Wang et al., 1992; Hu and Song, 2002; Zhang et al., 2006). The BSF, about 40 km in length, was formed as the important component of a basement-involved thrust system in the western part of the Yanshan structural belt during the late Mesozoic (Zhang et al., 2006). In a map view, the Shangyi Basin appears as a salient projecting to the east.

The basement rocks are mostly exposed on the northern, western and southern parts of the study area (**Figure 2A**). Among them, the Neoarchean Hongqiyingzi Complex (ca. 2.53 Ga; Liu et al., 2007; Peng et al., 2012) is exposed in the north of the study area, and consists predominantly of the biotite plagioclase gneiss, biotite granulite, garnet-bearing biotite schist, plagioclase amphibolite and a small amount of quartzite, marble. The Paleoproterozoic Khondalite (ca. 2.0 Ga; Dong et al., 2013) is present in the west part. In the southern part, the Neoarchean to Paleoproterozoic Huai'an Complex (ca. 2500–2000 Ma; Zhao et al., 2008; H. F. Zhang et al., 2011) is well-exposed and mainly composed of Tonalite–Trondhjemite–Granodiorite (TTG) rocks, granitic gneiss, mafic granulite and moyite. In addition, the Mesoproterozoic rocks, including carbonate rocks, quartzite, quartzose sandstone and shale, are present sporadically in the northern and southern sides of the basin (**Figure 2A**).

Most of the magmatic intrusions are exposed along the SPF (**Figure 2A**), and consists of Paleoproterozoic syenite, Late Paleozoic diorite and Early Mesozoic granite, diorite and

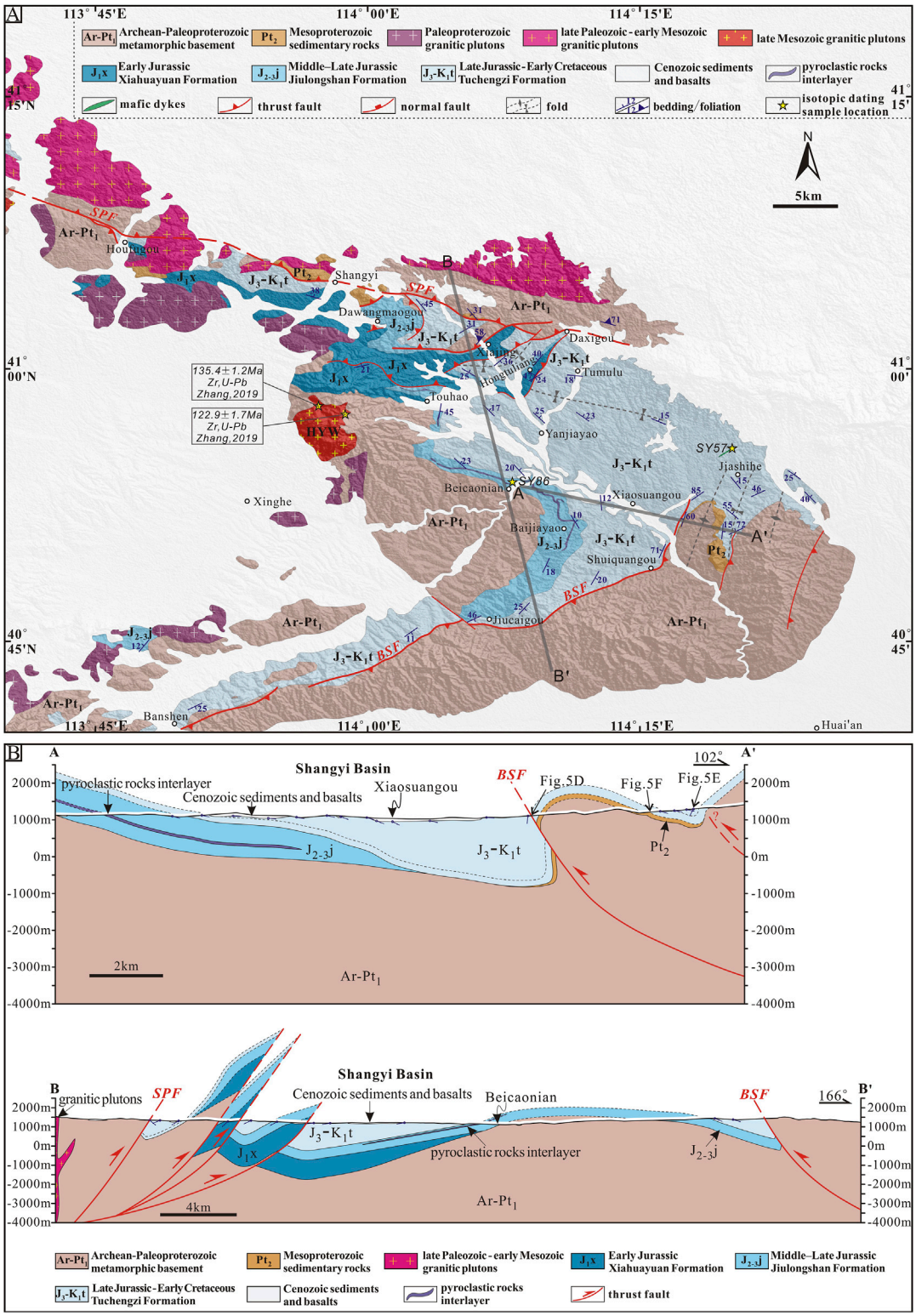

FIGURE 2 | (A) Geologic map of Shangyi area (modified after Xu et al., 2016). **(B)** Cross sections of A-A' and B-B'. *See* **Figure 1B** for location of this map. Locations of geochronological samples are shown on the map, and locations of some photos (**Figures 5D–F**) are also shown on the section A-A'. HYW, Huangyuwa granitic pluton. The rest figure captions are the same as **Figure 1B**.

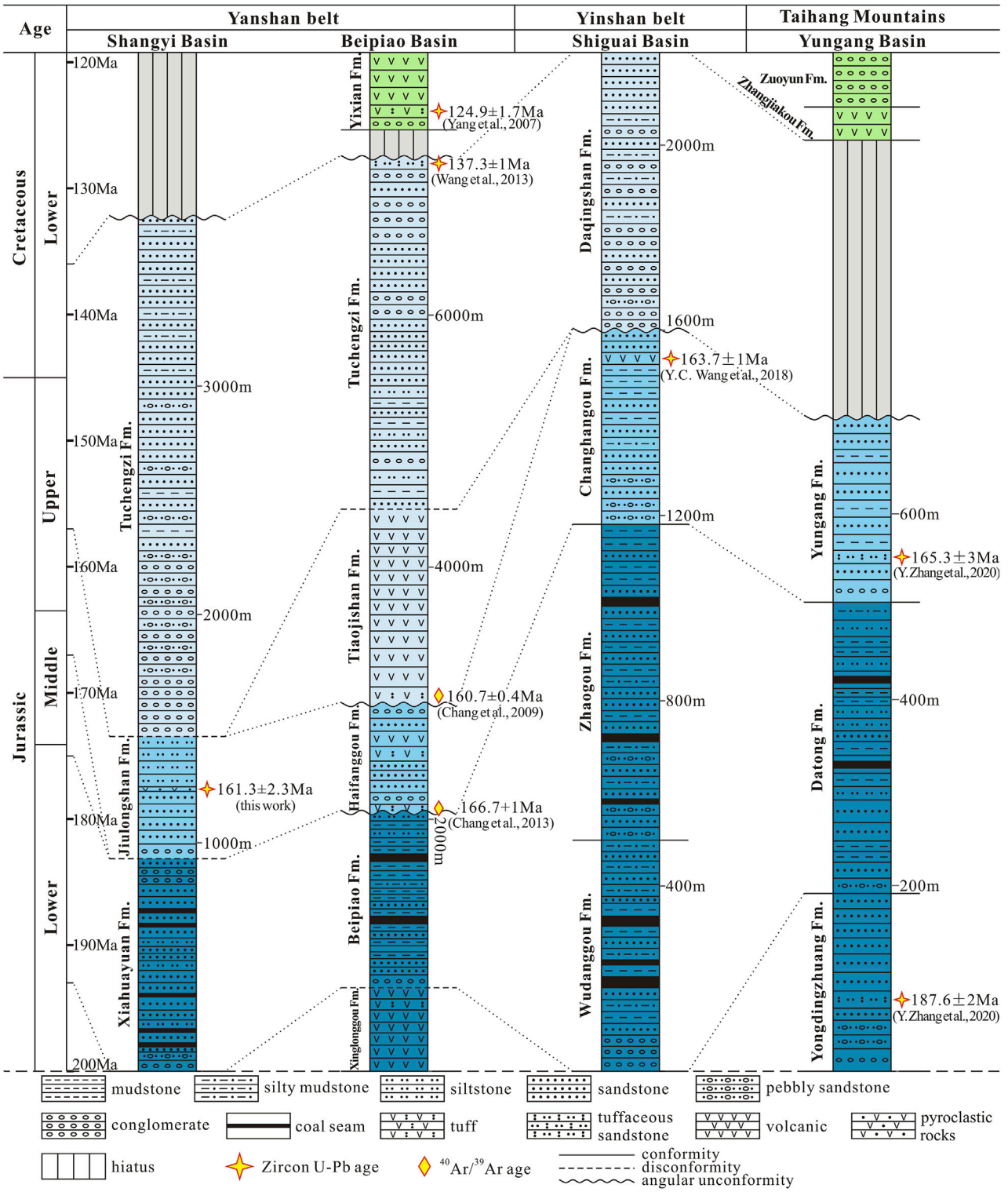

FIGURE 3 | Late Mesozoic stratigraphic units in the Shangyi Basin and its correlation with other typical late Mesozoic basins in the North China Carton. Beipiao, Shiguai, and Yungang basins were modified from J. Liu et al. (2015), Y.C. Wang et al. (2018) and Y. Zhang et al. (2020), respectively. The geochronological data of the late Mesozoic stratigraphic units in the Beipiao Basin were obtained from Yang et al. (2007), Chang et al. (2009, 2013) and Wang et al. (2013).

monzonite. Besides, minor amounts of Paleoproterozoic and Late Mesozoic intrusive bodies were emplaced in the western and southwestern basement rocks of the basin (**Figure 2A**). Among them, Late Paleozoic magmatism may be related to the closure of the Paleo-Asian Ocean (F. Wang et al., 2011). Recent research shows that the Huangyuwa granitic pluton, located about 10 km to the northeast of Xinghe, formed at 135–123 Ma, and it represents the product of magmatic activity in the Early Cretaceous (Zhang, 2019).

The basin Mesozoic stratigraphic sequence, in ascending order, comprises the Early Jurassic Xiahuayuan Formation, the Middle-Late Jurassic Jiulongshan Formation and the Late Jurassic–Early Cretaceous Tuchengzi Formation (**Figure 3**). The Xiahuayuan Formation present in the north part of the basin is characterized by a set of coal-bearing terrigenous sedimentation unit, which contains plentiful paleontological fossils, and it unconformably overlies the Khondalite series in the northwest side (**Figure 2A**). The Jiulongshan Formation is a set of variegated fluvial deposition accompany with small amount of basaltic andesite and pyroclastic rocks, which is mainly distributed in Hongtuliang, Xiajing and Dawangmaogou, as well as in the west side of the basin (**Figure 2A**). It unconformably contact with the underlying Xiahuayuan Formation and basement rocks. The Tuchengzi Formation is marked by the purple-red coarse-grained clastic sediments and widely distributed in the north, east, south and middle part of the basin. And it usually unconformably overlies the underlying older rock units. However, the Tuchengzi Formation in the north and south edges of the basin is also covered by Precambrian strata due to the influence of the boundary faults (**Figure 2A**). Broadly speaking, the Shangyi Basin is similar in lithological association with other typical Mesozoic basins in the northern margin of the NCC (**Figure 3**). Nevertheless, it is worth mentioning that the late Mesozoic volcanic rocks, including the Late Jurassic Tiaojishan Formation, the Early Cretaceous Zhanjiakou Formation and Yixian Formation are absent in our study area (**Figure 3**).

In addition, the Cenozoic stratigraphic units are widespread in the north of the SPF, the eastern side of the basin and the west of Xinghe. A large area of the Miocene clastic deposits and basalt are unconformable contact with the underlying pre-Cenozoic strata in the easternmost region.

Previous studies have revealed that the evolution of the Shangyi Basin was controlled by the SPF. Relevant investigations, such as the basin-fill sequence, sedimentary environment, and lithofacies palaeogeography, have been conducted (He et al., 2008; P. Zhang et al., 2014; Xu et al., 2016). Whereas, not enough attention was paid to the research of the multi-phase activity characteristics of the basin-controlling faults and the evolution of regional tectonic stress, as well as the effective isotope chronological constraints on the Late Mesozoic strata of the basin.

METHODOLOGY

Stress Inversion of Fault-slip Vectors

We can determine the stress tensor associated with fault movements by analysing fault nature and slip direction. Considering that fault slip data, including dip directions and angles of fault planes, pitch directions and angles of striations, and strike-slip directions, are easy to obtain, this method has been extensively applied to the study of tectonic evolution (Angelier, 1979, 1984; Delvaux et al., 1995; Delvaux and Sperner, 2003; Zhang et al., 2003; Allmendinger et al., 2012; Riller et al., 2017; Lin et al., 2015; Shi et al., 2015, 2020; B.; Zhang et al., 2020). The stress inversion method is usually based on the Wallace-Bott hypothesis, which suggests that the fault-slip vector (s) is parallel to the orientation of the maximum shearing stress (τ) under the influence of a regional uniform stress tensor (Wallace, 1951; Bott, 1959). Some other conditions also need to be considered, for example *1*) the stress field remain constant during a tectonic event (Angelier, 1979); *2*) the faults do not interfere with each other, with no rotation of the fault planes (Lacombe, 2012); and *3*) the protoliths of the deformed rocks are homogeneous and isotropic (Lacombe, 2012). In practice, there is usual an angle between the slip vector (s) and shear stress vector (τ). Therefore, this angle should be kept as small as possible so that the stress tensor we get is more accurate (Chen and Shi, 2015). The stress state or stress ellipsoid can be expressed by three principal stress axes (maximum (σ_1), intermediate (σ_2), and minimum (σ_3) stresses, where $\sigma_1 > \sigma_2 > \sigma_3$) and stress difference ratio ($R = (\sigma_2 - \sigma_3)/(\sigma_1 - \sigma_3)$, $0 \leq R \leq 1$). Theoretically, we need at least four independent fault-slip data to calculate a stress field (Etchecopar et al., 1981; Chen and Shi, 2015; B. Zhang et al., 2020).

In this work, we use Win-Tensor software (Delvaux et al., 1995; Delvaux and Sperner, 2003) for paleo-stress inversion. 314 fault-slip data were obtained from 34 observation sites in the field (**Table 1**). The relative sequences of multi-stage tectonic deformation can be determined by identifying the youngest strata that involved in various stages of deformation, by analyzing the superposition relationships of multiple slip vectors on a single fault surface, and by observing the cross-cutting relationships of truncated fault planes (Shi et al., 2015, 2020). According to the above analysis, together with the attitude of the fold hinges and the angular bisector orientations of the X-type conjugate shear fractures from different strata, we are able to reconstruct the evolutionary sequence of the late Mesozoic tectonic stress field in the Shangyi Basin.

Balanced Cross-section Restoration

In order to carry out the quantitative analysis to tectonic deformation of the basin, we use the technique of balanced cross-section to restore the deformation and structure to its initial state based on the reliable geologic section and related geometrical rules (Dahlstrom, 1969; Hosseck, 1979; Li et al., 2011; Zhang et al., 2011; Nakapelukh et al., 2017; Y. Zhang et al., 2020). Because of the lack of seismic and borehole data in our study area, we mainly based our cross-sections on detailed field geological investigations. Generally speaking, the cross-sections should theoretically be kept orthogonal to the strikes and axes of faults and folds (or parallel to the direction of regional principal stress) (Hosseck, 1979; Song, 1985) so that the deformation behavior and the amount of shortening can be defined more accurately. Taking into account the major structural features of the basin, the sections A-A' with NW-

TABLE 1 | Slip vectors on fault planes measured in the Shangyi Basin and their paleostress fields.

Site	Longitude (E)	Latitude (N)	Stratigraphy-lithology	Vector number	σ_1 (az°/pl°)	σ_2 (az°/pl°)	σ_3 (az°/pl°)	R
NW-SE compressive stress field								
SY06-1	114°02′52.79″	40°45′40.88″	J_3-K_{1t} sandy conglomerate	4	284/10	049/74	192/13	0.5
SY07-1	114°05′58.10″	40°46′11.86″	J_3-K_{1t} sandy mudstone	12	137/25	259/49	031/31	0.28
SY09	114°09′16.10″	40°46′43.12″	J_3-K_{1t} sandy mudstone	4	340/09	243/39	080/50	0.29
SY11	114°16′22.73″	40°49′58.31″	J_3-K_{1t} sandy mudstone	15	303/16	045/35	193/50	0.47
SY14	114°15′07.03″	40°48′54.75″	J_3-K_{1t} sandstone	4	152/00	242/50	062/40	0.5
SY15	114°16′04.22″	40°49′16.86″	J_3-K_{1t} sandstone	4	109/07	016/18	218/71	0.5
SY18	114°12′38.08″	40°48′29.54″	J_3-K_{1t} sandy mudstone	4	137/13	352/74	229/09	0.5
SY26	114°17′20.19″	40°51′42.46″	J_3-K_{1t} sandstone	16	135/00	045/05	225/85	0.43
SY28	114°20′11.52″	40°52′02.01″	J_3-K_{1t} sandstone	7	141/14	234/08	354/74	0.5
SY29	114°20′23.82″	40°51′02.33″	J_3-K_{1t} sandy mudstone	14	330/07	239/05	117/82	0.46
SY32-1	114°19′27.65″	40°51′03.46″	J_3-K_{1t} conglomerate	5	310/18	041/04	142/71	0.5
SY39-1	113°57′26.41″	41°04′51.55″	J_3-K_{1t} sandy conglomerate	7	321/02	060/77	230/13	0.64
SY40-1	113°57′08.09″	41°03′58.99″	J_{1x} conglomerate	4	339/01	248/62	069/28	0.5
SY42-1	114°07′39.31″	41°02′17.93″	fault zone	6	304/01	034/01	166/88	0.42
SY43	114°00′44.38″	41°03′52.95″	fault zone	4	321/02	230/20	057/70	0.5
SY44-1	114°03′02.66″	41°03′30.74″	J_3-K_{1t} conglomerate	4	319/19	060/29	201/54	0.62
SY45-1	114°05′14.18″	41°02′32.42″	J_3-K_{1t} conglomerate	4	140/02	038/79	230/10	0.62
SY48-1	114°07′09.07″	41°00′36.39″	J_{1x} sandstone	5	328/11	234/22	082/65	0.3
SY49-1	114°09′29.66″	41°00′27.75″	$J_{2\text{-}3j}$ sandy conglomerate	10	120/00	210/31	029/59	0.28
SY58	114°05′50.59″	41°03′01.78″	Pt_2 dolomite	5	146/17	040/43	252/42	0.44
SY68-1	114°11′37.76″	41°00′42.40″	J_3-K_{1t} conglomerate	6	155/24	049/32	275/48	0.5
SY86	114°08′03.36″	40°53′45.65″	$J_{2\text{-}3j}$ pyroclastic rocks	5	339/03	246/03	066/86	0.42
NW-SE extensional stress field								
SY07-2	114°05′58.10″	40°46′11.86″	J_3-K_{1t} sandy mudstone	7	267/86	034/03	125/03	0.57
SY10	114°14′13.59″	40°49′24.82″	J_3-K_{1t} sandstone	5	282/64	058/19	154/17	0.5
SY21	114°11′32.30″	40°51′34.53″	$J_{2\text{-}3j}$ andesite	4	263/62	027/17	124/22	0.5
SY31	114°20′12.15″	40°51′03.62″	J_3-K_{1t} sandy mudstone	4	224/51	044/39	314/00	0.57
SY34-1	113°47′46.61″	40°44′42.01″	$J_{2\text{-}3j}$ conglomerate	4	220/60	036/30	127/02	0.67
SY40-2	113°57′08.09″	41°03′58.99″	J_{1x} conglomerate	7	226/53	062/36	326/08	0.8
SY44-2	114°03′02.66″	41°03′30.74″	J_3-K_{1t} conglomerate	4	188/68	075/09	342/20	0.5
SY45-2	114°05′14.18″	41°02′32.42″	J_3-K_{1t} conglomerate	5	018/87	218/03	128/01	0.44
SY48-2	114°07′09.07″	41°00′36.39″	J_{1x} sandstone	5	360/83	213/06	122/04	0.33
SY49-2	114°09′29.66″	41°00′27.75″	$J_{2\text{-}3j}$ sandy conglomerate	42	050/76	217/14	307/03	0.49
SY50-1	114°09′42.48″	41°01′39.32″	J_3-K_{1t} conglomerate	5	045/85	219/05	309/01	0.89
SY68-2	114°11′37.76″	41°00′42.40″	J_3-K_{1t} conglomerate	11	333/75	237/01	147/15	0.64
SY78	114°06′24.19″	40°58′25.23″	J_3-K_{1t} pebbly sandstone	4	003/71	236/12	143/15	0.38
NE-SW compressive stress field								
SY05	40°45′28.30″	40°58′25.23″	J_3-K_{1t} sandy conglomerate	8	208/02	305/77	117/13	0.5
SY06-2	114°02′52.79″	40°45′40.88″	J_3-K_{1t} sandy conglomerate	6	206/05	340/83	115/05	0.5
SY16	114°08′43.06″	40°46′47.24″	J_3-K_{1t} sandy mudstone	6	030/12	181/76	298/07	0.5
SY20	114°12′05.95″	40°51′35.66″	$J_{2\text{-}3j}$ pebbly sandstone	6	059/01	325/79	150/11	0.42
SY27	114°18′29.78″	40°52′55.12″	J_3-K_{1t} sandstone	6	200/28	056/57	299/16	0.5
SY36	113°52′31.15″	40°41′47.95″	J_3-K_{1t} sandy conglomerate	4	214/03	306/39	120/51	0.62
SY42-2	114°07′39.31″	41°02′17.93″	fault zone	5	073/03	341/44	166/46	0.5
SY48-3	114°07′09.07″	41°00′36.39″	J_{1x} sandstone	4	039/04	308/09	155/80	0.5
SY68-3	114°11′37.76″	41°00′42.40″	J_3-K_{1t} conglomerate	5	019/15	252/66	114/18	0.3
SY71	114°10′42.61″	41°02′01.83″	fault zone	7	034/11	301/17	156/69	0.45

σ_1, σ_2, σ_3 correspond to maximum, intermediate, and minimum principal stresses, respectively; az°, azimuth; pl°, plunge; $R = (\sigma_2-\sigma_3)/(\sigma_1-\sigma_3)$, the data was obtained by using Win_Tensor 5.8.9 (http://damiendelvaux.be/Tensor/WinTensor/win-tensor_download.html); Pt_2, Mesoproterozoic; J_{1x}, Lower Jurassic Xiahuayuan Formation; $J_{2\text{-}3j}$, Upper-Middle Jurassic Jiulongshan Formation; J_3-K_{1t}, Upper Jurassic-Lower Cretaceous Tuchengzi Formation.

SE-trending and B-B' with NNW-SSE-trending were selected for balancing and restoration (**Figures 2A,B**). Here we took the 2D-Move software to restore the deformation and estimate the crustal shortening. Meanwhile, the layer length conservation principle and plane strain should be considered during the analysis process (Dahlstrom, 1969; Li et al., 2011; Li et al., 2019).

LA-ICP-MS Zircon U-Pb Dating

To constrain the timing of tectonic deformation in the Shangyi Basin, we analyzed zircon grains from two selected rock samples (for sample locations, *see* **Figure 2A**) using LA–ICP–MS U–Pb dating. Zircon grains were extracted from crushed blocks using heavy liquid and magnetic separation techniques. Zircons were handpicked under a binocular microscope, mounted in epoxy resin, polished to expose approximately half of the grains, and gold coated. Cathodoluminescence (CL) images of zircon grains were acquired using an Analytical Scanning Electron Microscope (JSM–IT100) connected to a GATAN MINICL system. LA–ICP–MS zircon U–Pb dating was conducted at the Key

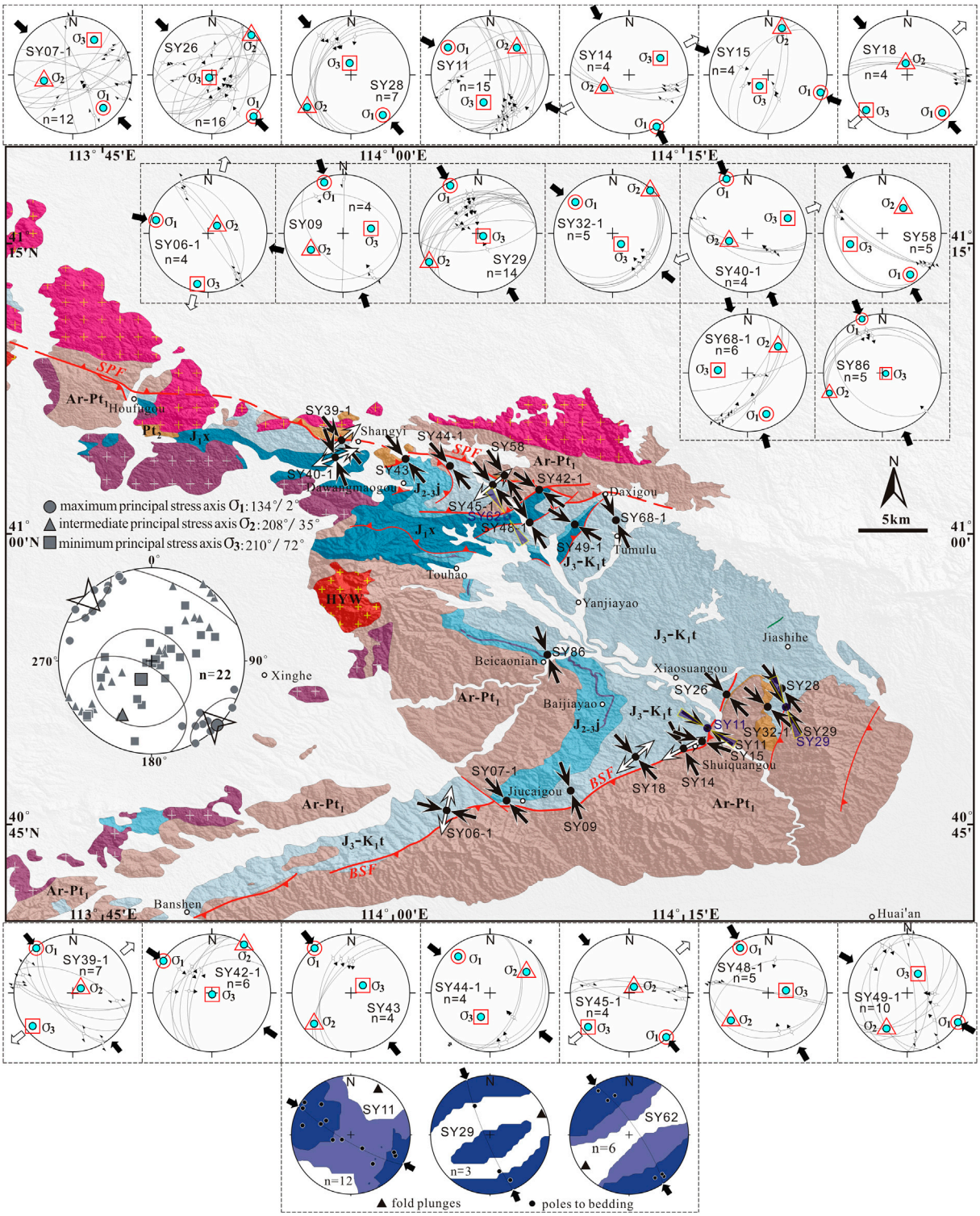

FIGURE 4 | Stereographic plots for the NW-SE compressive stress field in Shangyi area, derived from analysis of fault-slip data and folds (figure captions are the same as **Figures 1B**, **2A**). Principal stress axes (σ_1, σ_2 and σ_3) of regional stress field are also shown on the map. Lower hemisphere, equal-area projections.

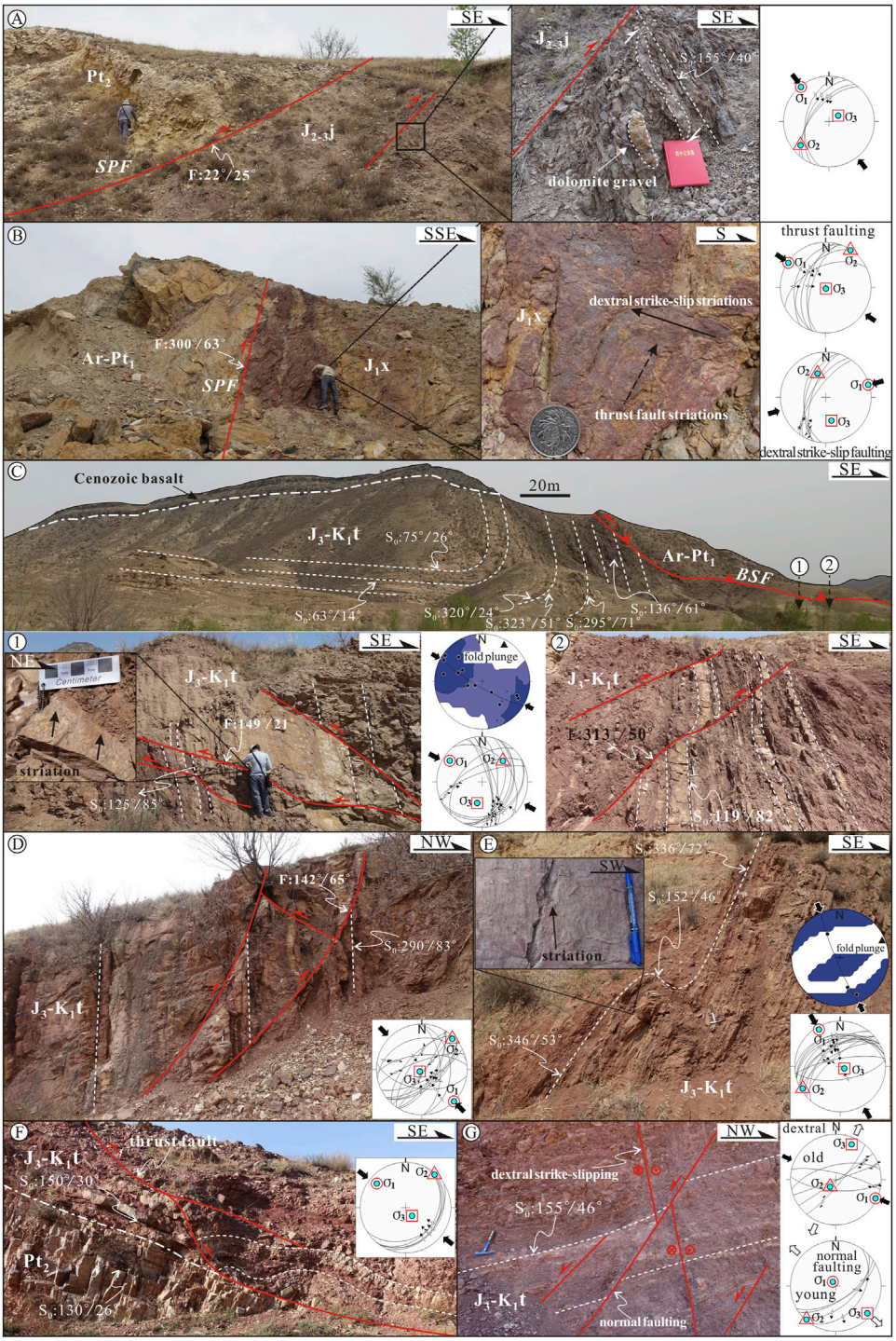

FIGURE 5 | Representative outcrop photographs related to regional NW-SE compression. **(A)** Mesoproterozoic carbonate rocks are overthrust southeastward over the Jiulongshan Formation along the Shangyi-Pingquan Fault (SPF) accompanied by related drag fold exposed in the footwall. **(B)** Two sets of striations, including dip-direction striations with reverse faulting and sub-horizontal dextral strike-slip striations, are simultaneously exposed on one fault surface in the Xiahuayuan Formation sandstones from the footwall of the SPF, corresponding to NW-SE and NE-SW compression, respectively. **(C)** The basement rocks are overthrust northwestward onto the Tuchengzi Formation along the Banshen-Shuiquangou Fault (BSF), accompanied with an intermediate-scale overturned syncline developed in the footwall. **(D)** Approaching the BSF, the Tuchengzi Formation show nearly upright. **(E)** Outcrop-scale ENE-trending fold accompanied with interlayer slip. **(F)** A SE-dipping reverse fault with low dip angle has occurred along the unconformable contact between the Tuchengzi Formation conglomerates and the Mesoproterozoic quartz sandstones. **(G)** Two groups of faults crop out in the Tuchengzi Formation sandstones, including NE-striking dextral strike-slip and SE-dipping normal faults, corresponding to NW-SE compression and NW-SE extension, respectively. All the structural measurements in this work were expressed by dip direction and dip angle. Lower hemisphere, equal-area projections.

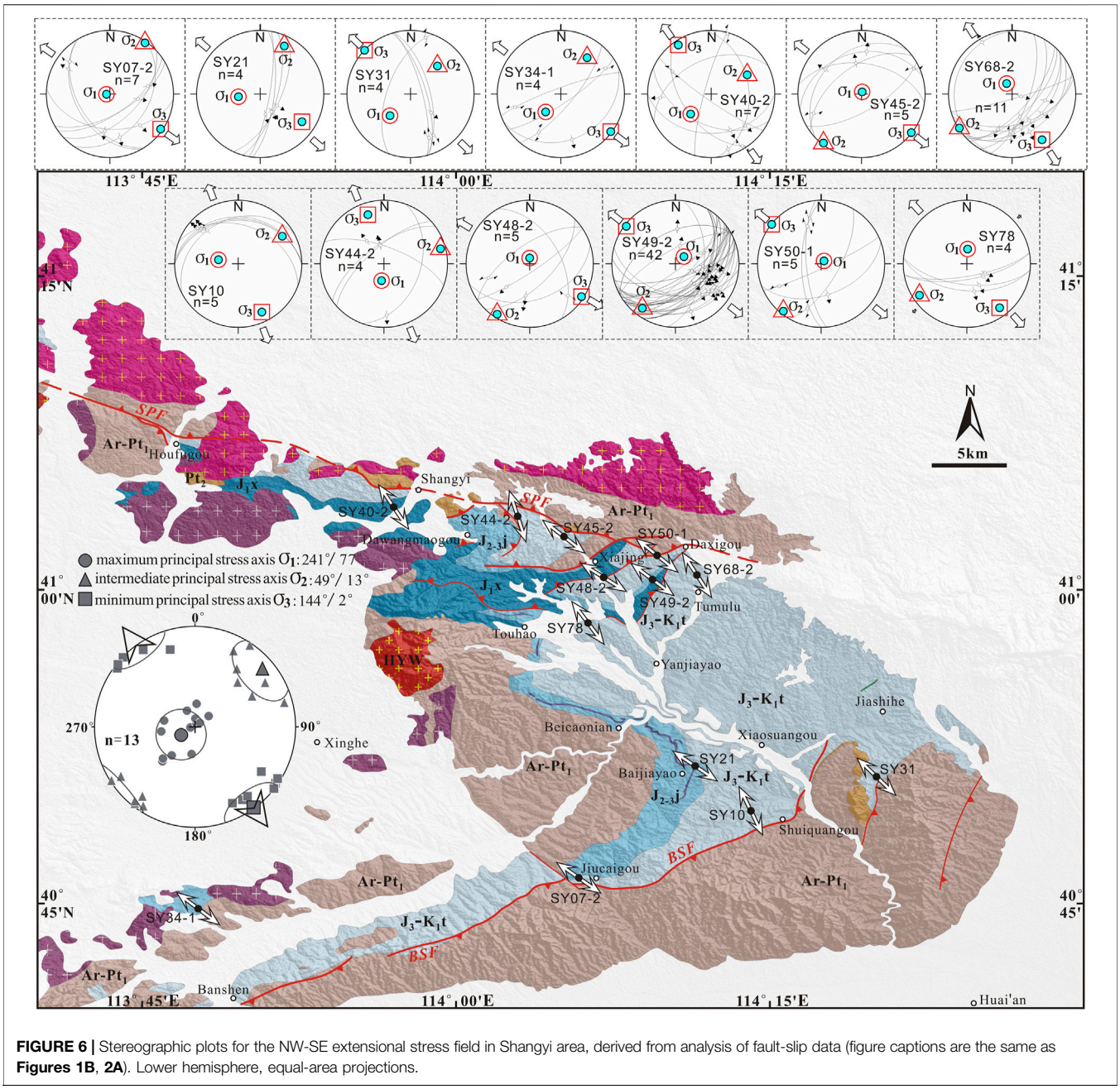

FIGURE 6 | Stereographic plots for the NW-SE extensional stress field in Shangyi area, derived from analysis of fault-slip data (figure captions are the same as **Figures 1B**, **2A**). Lower hemisphere, equal-area projections.

Laboratory of Paleomagnetism and Tectonic Reconstruction, Ministry of Natural Resources, Beijing. The spot size and laser frequency were set to 32 μm and 5 Hz, respectively. Zircon 91500 was taken as an external standard for the U–Pb dating, and glass NIST610 was used as a standard for the trace-element calibration. The ICPMSDataCal software was used to calibrate the trace-element analysis and U–Pb dating (Liu et al., 2008, 2010). Weighted mean calculations and concordia diagrams were acquired using Isoplot/Ex_ver3 (Ludwig, 2003).

STRUCTURAL ANALYSIS IN THE SHANGYI BASIN

Major Faults and Folds

The major faults and related folds are exposed along the north and south edges of the basin. Along the northern boundary of the basin, the SPF from west of Houfugou to east of Daxigou is striking WNW-ESE and dipping towards the north or north-northeast, in spite of its whole orientation in the Yanshan belt as ~E-W (**Figures 1B**, **2A**). Along the SPF, Neoarchean-Paleoproterozoic

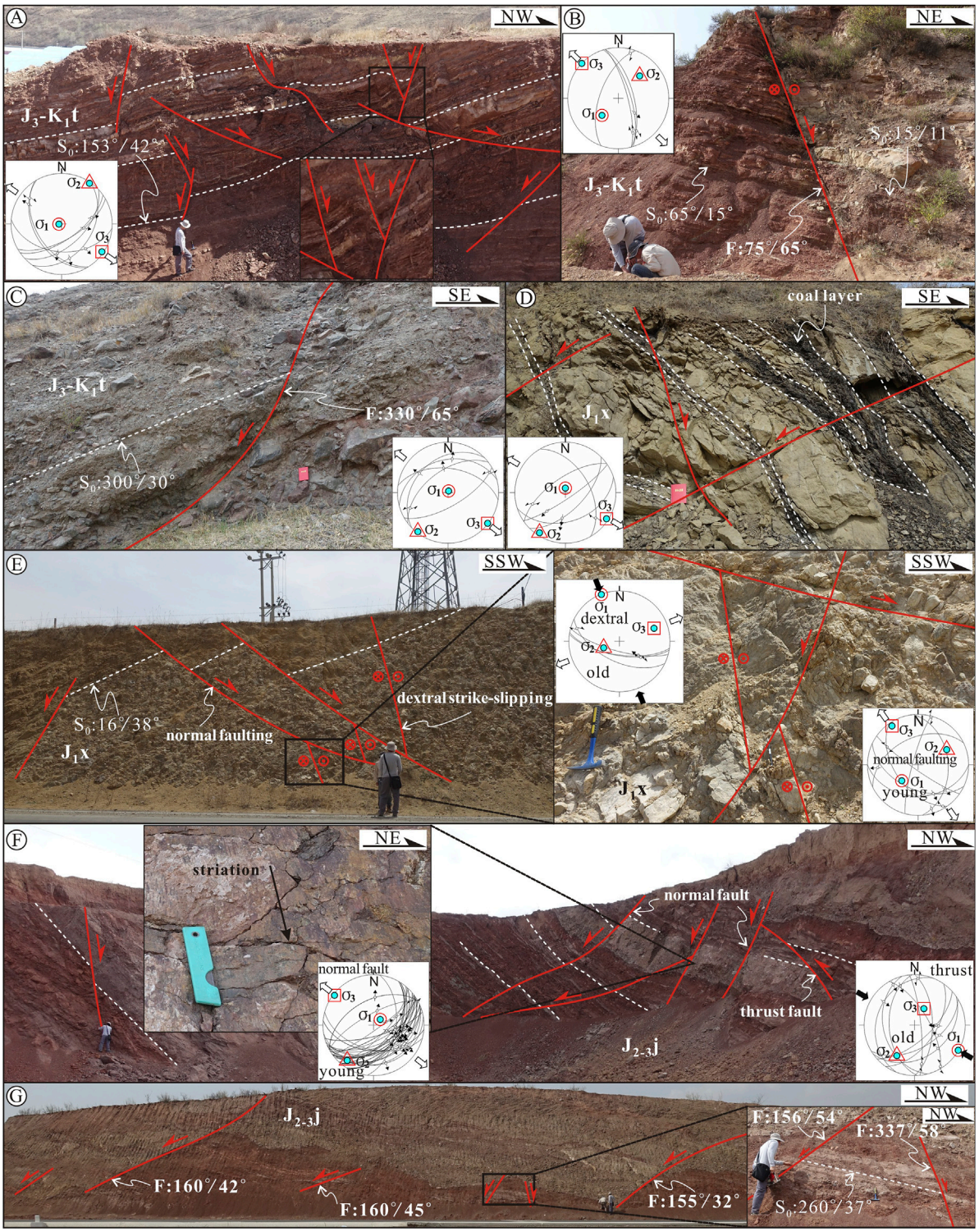

FIGURE 7 | Representative outcrop photographs related to regional NW-SE extension. Photo **(A–C)** shows that some small-scale normal and strike-slip faults are developed in the Tuchengzi Formation and reflect NW-SE extensional deformation. **(D)** At the south of Xiajing, the later SE- or NW-dipping normal faults dislocate the early tight folds in the coal-bearing sandstones in the Xiahuayuan Formation. **(E)** Two groups of faults crop out in the Xiahuayuan Formation sandy conglomerates at the southwest of Shangyi. And the dextral strike-slip faults are cut by the SSW-dipping transtensional faults, corresponding to NW-SE compression and NW-SE extension, respectively. **(F)** Two-phase faults are exposed in the Jiulongshan Formation at the northeast of Hongtuliang, and the early NW-dipping reverse faults are truncated by the lather SE-dipping normal faults, corresponding to NW-SE compression and NW-SE extension, respectively. **(G)** Some NW- and SE-dipping extension faults and well-developed horst are marked in the Jiulongshan Formation at the northeast of Hongtuliang. Lower hemisphere, equal-area projections.

basement and a few Mesoproterozoic caprock are overthrust southward onto Late Mesozoic strata. Within the footwall of the SPF, near Dawangmaogou, Xiajing and Hongtuliang, some ~E-W- and NE-striking secondary thrusts show tectonic vergence towards the south (or the southeast). These secondary faults extend towards the northeast and eventually merge into the SPF (**Figure 2A**), indicating that the former are controlled by the latter. In the south margin, the BSF from Banshen to Shuiquangou is striking NE, whereas east of Shuiquangou, its direction changes into NNE (**Figure 2A**), and it finally disappeared in the Tuchengzi Formation of the east of Xiaosuangou. The BSF is generally steeply dipping (>60°) towards the southeast. Along the BSF, the basement rocks are thrust northwestward over the Tuchengzi Formation (**Figure 2B**). According to the variation trend of the attitude of the rock stratum in geological map, some folds with the NE-trending axes are mainly observed in the north and south parts of the basin, showing the asymmetric syncline or anticline controlled by the boundary faults (**Figure 2B**). Additionally, a WNW-trending gentle syncline occurs between Yanjiayao and Tumulu (**Figure 2A**), which represents a structural style different from the asymmetric folds described above.

Multi-phase Deformations and Paleo-stress Fields

Based on detailed field measurements from the Shangyi Basin, together with the superposition and cross-cutting relationships of different structures, three-stage deformation can be identified. In this part, we mainly introduced the structural deformation characteristics of each stage, as well as the corresponding inversion results of fault slip data. Relevant interpretations of their deformation sequences were presented in the Discussion section.

First Set of Structures: NW-SE Compression

We collected abundant evidence associated with this compression from 23 sites in the margins and interior of the basin (**Figure 4**). On the northern edge, the Neoarchean Hongqiyingzi Complex and the Mesoproterozoic quartz sandstones and carbonate rocks are usually thrust over the late Mesozoic strata along the SPF (**Figures 5A,B**). Slickensides and steps of the faults, asymmetric folds and fault-related drag structures all indicate a reverse faulting with the top-to-the-SE slip sense, and a NW-SE maximum principal stress (σ_1) inferred by relevant fault-slip vectors (**Figures 5A,B**). On the southern fringe, approaching the northeast of Shuiquangou (site SY11) (**Figure 4**), a medium-scale NE-trending asymmetric syncline unconformably covered by the near-horizontal Cenozoic basalts can be noticed in the purple-red sandstones (Tuchengzi Formation) from the lower plate of the BSF (**Figure 5C**). The southeast limb of the syncline is short and sub-vertical (even overturned), but its northwest limb is long and gentle, which suggests the BSF has the kinematics with the top-to-the-NW slip sense (**Figure 2B**). Some other small-scale folds with the sub-horizontal NE-oriented hinges can be observed in the Tuchengzi Formation from the south of Jiashihe (site SY29) (**Figures 4**, **5E**). Furthermore, a SE-dipping reverse fault with low dip angle has occurred along the unconformable contact between the conglomerates of the Tuchengzi Formation and the Mesoproterozoic quartz sandstones at the site SY32 (**Figures 4**, **5F**). The fault-slip data collected along the BSF and adjacent secondary fractures were used for stress inversion, defining a uniform NW-SE maximum principal stress (σ_1) (**Figures 4**, **5C–G**). We made a systematic analysis to 149 fault-slip data points from 22 sites (**Table 1**) and gained a stress regime with a regional 134°/02° for σ_1, 208°/35° for σ_2, and 210°/72° for σ_3 (**Figure 4**), indicating a stress regime dominated by NW-SE compression.

In addition, two sets of striations can be recognized on the same NW-dipping fault plane in the sandstones (Xiahuayuan Formation) from the footwall of the SPF. One group is marked by thrust faulting and the other group is characterized by dextral strike-slip faulting, corresponding to the NW-SE and NE-SW principal compressive stresses, respectively (**Figure 5B**). Approaching the west of Jiucaigou, two-phase faults were identified in the Tuchengzi Formation, and the early ENE-striking dextral strike-slip faults were cut by the later SE-dipping normal ones, corresponding to a NW-SE principal compressive stress and a NW-SE principal tensile stress, respectively (**Figure 5G**).

Second Set of Structures: NW-SE Extension

Remarkable structural styles related to the second set of structures may not be easily discernible on the map, but we still obtained some related clues from 13 artificial and natural outcrops (**Figures 6**, **7A–G**). As the same with the first set of structures, all the late Mesozoic clastic sediments filled in the basin were involved in this extensional event, expressed by a series of SE- or NW-dipping normal faults (**Figures 7A,C,D,F,G**), transtensional faults (**Figures 7B,E**), and some typical grabens and horsts (**Figure 7G**). Here the systematic analysis from 107 fault-slip vectors (**Table 1**) shows a regional maximum principal stress axis (σ_1) at 241°/77°, intermediate principal stress axis (σ_2) at 049°/13°, and minimum principal stress axis (σ_3) at 144°/02° (**Figure 6**), suggesting a stress regime of NW–SE extension.

Moreover, some evidence reveals that the early structures were reworked by this extensional deformation, for example some NW- or SE-dipping normal faults dislocated the early NE-trending tight folds (**Figure 7D**) and cut the pre-existing NE-striking reverse faults (**Figure 7F**). At site SY40, near the southwest of Shangyi County, two groups of faults developed in the Xiahuayuan Formation with different activity times, where the early WNW-striking dextral strike-slip faults were severed by the later SSW-dipping transtensional faults, corresponding to a NW-SE compressive stress state and a NW-SE stretching stress state, respectively (**Figure 7E**).

Third Set of Structures: NE-SW Compression

In our research area, the third set of structural deformation is weaker than the previous two sets of structures that we described above in terms of the scale and activity intensity. Related deformational behaviors were found from 11 field outcrops (**Figures 8**, **9A–F**), expressed by some miniature transpressional faults (**Figures 9A,E**), X-type conjugate shear fractures (**Figure 9B**), conjugate strike-slip faults (**Figures 9C,D**), and outcrop-scale folds. Both the acute-angled bisector direction of the X-type conjugate shear fractures and the azimuth of the horizontal orthogonal line of fold axes are NE- or SW-directed,

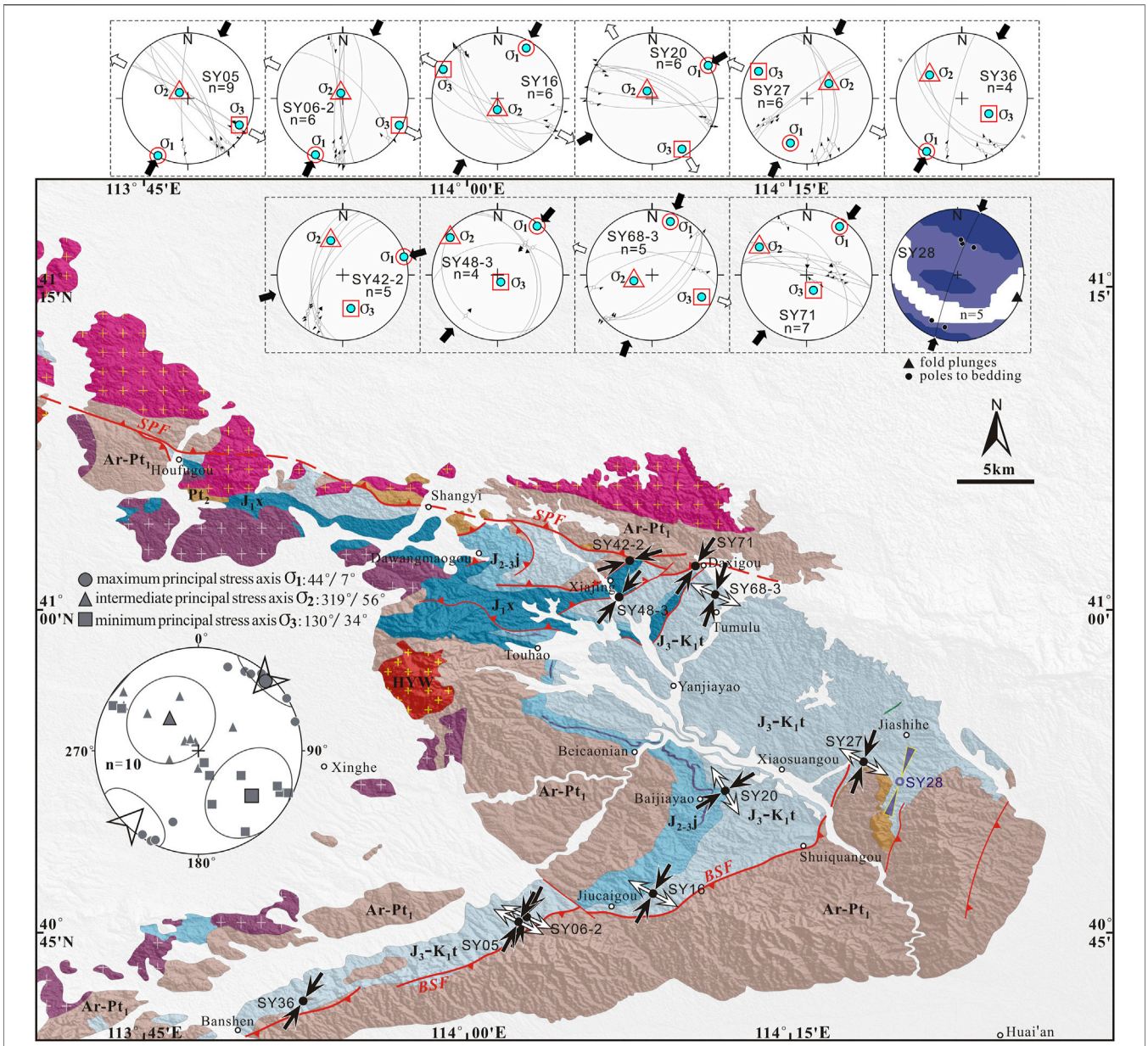

FIGURE 8 | Stereographic plots for the NE-SW compressive stress field in Shangyi area, derived from analysis of fault-slip data and folds (figure captions are the same as **Figures 1B**, **2A**). Lower hemisphere, equal-area projections.

which also represents the orientation of maximum principal stress axis (σ_1). The systematic analysis from 58 fault-slip vectors (**Table 1**) indicates a regional stress field with σ_1 of 044°/07°, σ_2 of 319°/56°, and σ_3 of 130°/34° (**Figure 8**), implying a territorial NE-SW principal compressive stress.

Moreover, at the north of Tumulu (site SY68), a few evidence of multiphase tectonic activity is recorded in the conglomerates of the Tuchengzi Formation. The early SE-dipping normal faults were dislocated by the later N-dipping sinistral strike-slip faults. Inversion of fault-slip data shows that these two deformations represent separately the influence of the NW-SE extension and NE-SW compression (**Figure 9F**).

ANALYSES OF CROSS-SECTION RESTORATION AND CRUSTAL SHORTENING RATIO

The geological cross-sections A-A' and B-B' (**Figures 2A,B**) are restored, aiming to estimate crustal shortening in the study area due to the NW-SE compressive stress field. Since the youngest strata involved in the NW-SE compressional deformation is the Tuchengzi Formation, which is widely distributed in the basin, we can take the lower boundary of the Tuchengzi Formation as the marker bed for cross-section restoration.

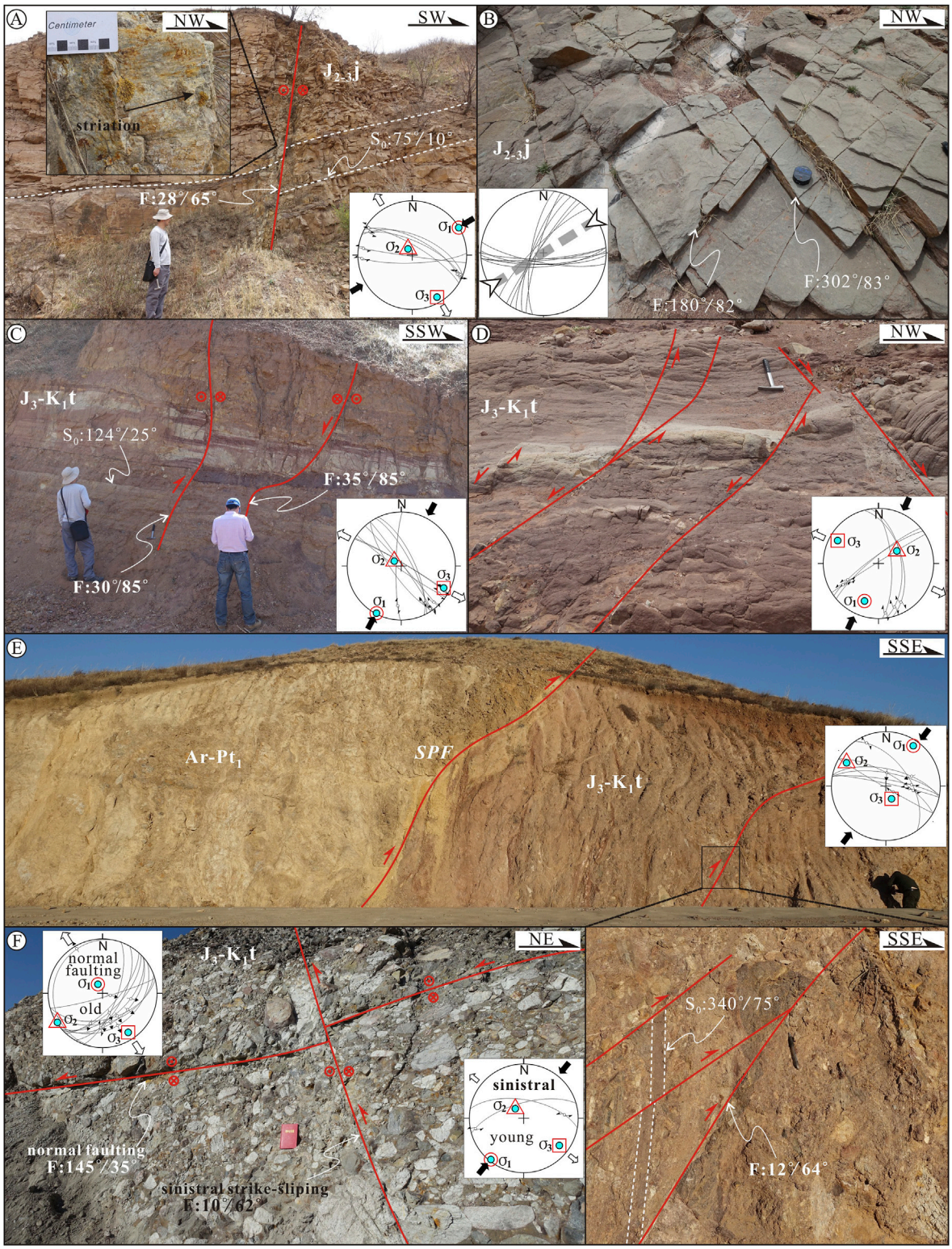

FIGURE 9 | Representative outcrop photographs related to regional NE-SW compression. **(A)** Outcrop-scale WNW-striking strike-slip fault crop out in the pebbly sandstones of the Jiulongshan Formation, and a NE-SW compressive stress obtained by inversion of fault-slip vectors. **(B)** The X-type conjugate shear fractures with NE-directed acute-angled bisector are developed in the Jiulongshan Formation sandstones. **(C,D)** Conjugate strike-slip faults associated with NE-SW compressional deformation are marked in the Tuchengzi Formation. **(E)** Near the west of Daxigou, evidence of faulting related to NE-SW compression is discovered in the Tuchengzi Formation sandy conglomerates from the footwall of the SPF. **(F)** Two-phase faults are exposed in the Tuchengzi Formation conglomerates at the north of Tumulu, and the SE-dipping normal faults are cut by NNE-dipping transpressional faults, corresponding to NW-SE extension and NE-SW compression, respectively. Lower hemisphere, equal-area projections.

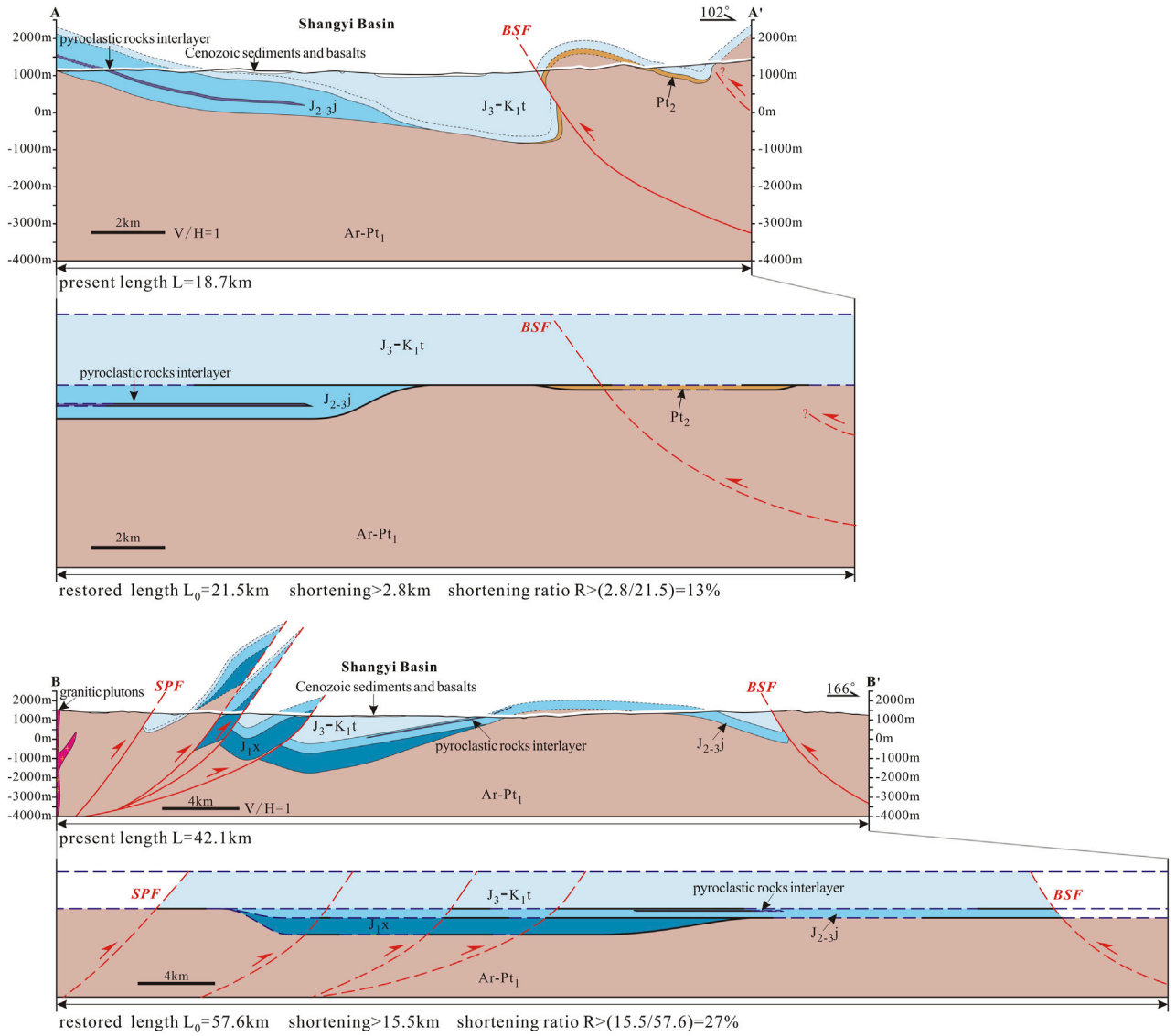

FIGURE 10 | The results of balance and restoration of the sections A-A' and B-B'. Subsurface geometries are largely schematic due to lack of geophysical data. The legends are the same as **Figure 2B**. The rest figure captions are the same as **Figure 1B**.

To make the operation easier, it is usually assumed that the same layer is a constant thickness along the entire section. However, our field investigations do not support such a hypothesis. For instance, in the section A-A', the stratigraphic sequence in the footwall of the BSF is successively the Neoarchean-Paleoproterozoic basement unit, the Jiulongshan Formation, and the Tuchengzi Formation from the bottom up, which is quite different from that in the hanging wall, including the basement rocks, the Mesoproterozoic quartz sandstones and the Tuchengzi Formation in ascending order (**Figures 2B**, **10**). The Jiulongshan Formation is only developed in the footwall of the BSF, which is absent in the upper wall. Here we can speculate that the palaeotopographical effect may trigger the pinch-out of the Jiulongshan Formation in the lower plate of the BSF and then may cause a directly unconformable contact between the Tuchengzi Formation and the underlying older strata. The similar case may occur in the Mesoproterozoic unit of the section A-A', as well as in other related strata of the section B-B' (**Figures 2B**, **10**). Therefore, taking the bottom boundary of the Tuchengzi Formation as the marker layer can avoid the above problem effectively. Besides, given the tectonic denudation, we can't confirm the original depositional thickness of the Tuchengzi Formation, and only replace it with the maximum layer thickness on the sections. Finally, the layer length conservation principle was used to estimate the minimum crustal shortening (Li et al., 2011). Additionally, we ignore the effects of the NW-SE extension and NE-SW compression, as these tectonic events generated limited reshaping of the present-day cross-sections (the sections A-A' and B-B').

Our results show that the present lengths of the sections A-A' and B-B' are independently 18.7 and 42.1 km, and their restored

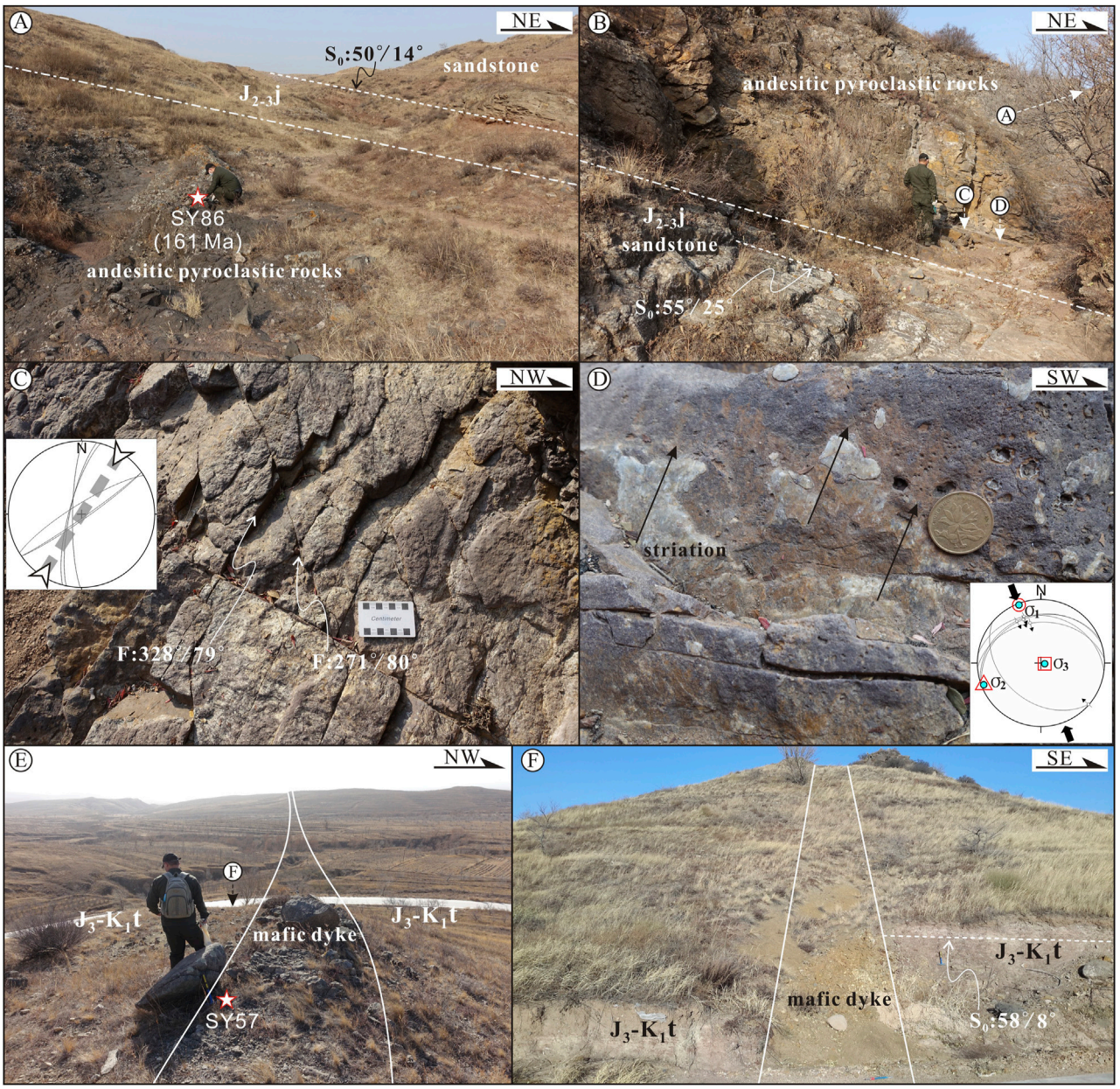

FIGURE 11 | Outcrop photographs of zircon U-Pb dating samples from Shangyi area. **(A)** Sample SY86 was collected from a pyroclastic interlayer within the sandstones of the Jiulongshan Formation near the Beicaonian in the west edge of the basin. The interlayer, along with surrounding strata, is gently inclined to the northeast. **(B)** The conformable contact between the pyroclastic interlayer and underlying sandstones. **(C)** The X-type conjugate shear fractures resulted from NE-SW compression are exposed on the pyroclastic rocks. **(D)** Fault striations associated with NW-SE compression are developed in the pyroclastic rocks. **(E)** Sample SY57 was acquired from a NE-trending mafic dike intruded into the sandstones (Tuchengzi Formation) at the north of Jiashihe. **(F)** The near-upright mafic dike is embedded in the subhorizontal Tuchengzi Formation sandstones. Lower hemisphere, equal-area projections.

lengths are separately 21.5 and 57.6 km, indicating their minimum shortening ratios are 13 and 27%, respectively (**Figure 10**). The crustal shortening was mainly accommodated by the boundary thrust faulting and internal folding of the basin. In addition, most of the deformation occurred in the north and south margins of the basin accompanied with weak tectonic response in the interior region. Combined with the space geometries and shortening ratios of the two cross-sections (**Figures 2A,B**, **10**), we discovered that the contribution of tectonic shortening from the north part of the basin obviously exceeded that from the south side.

GEOCHRONOLOGICAL RESULTS

Two rock samples were collected for zircon U-Pb dating to constrain the timing of deformation in the basin. Sample locations are shown

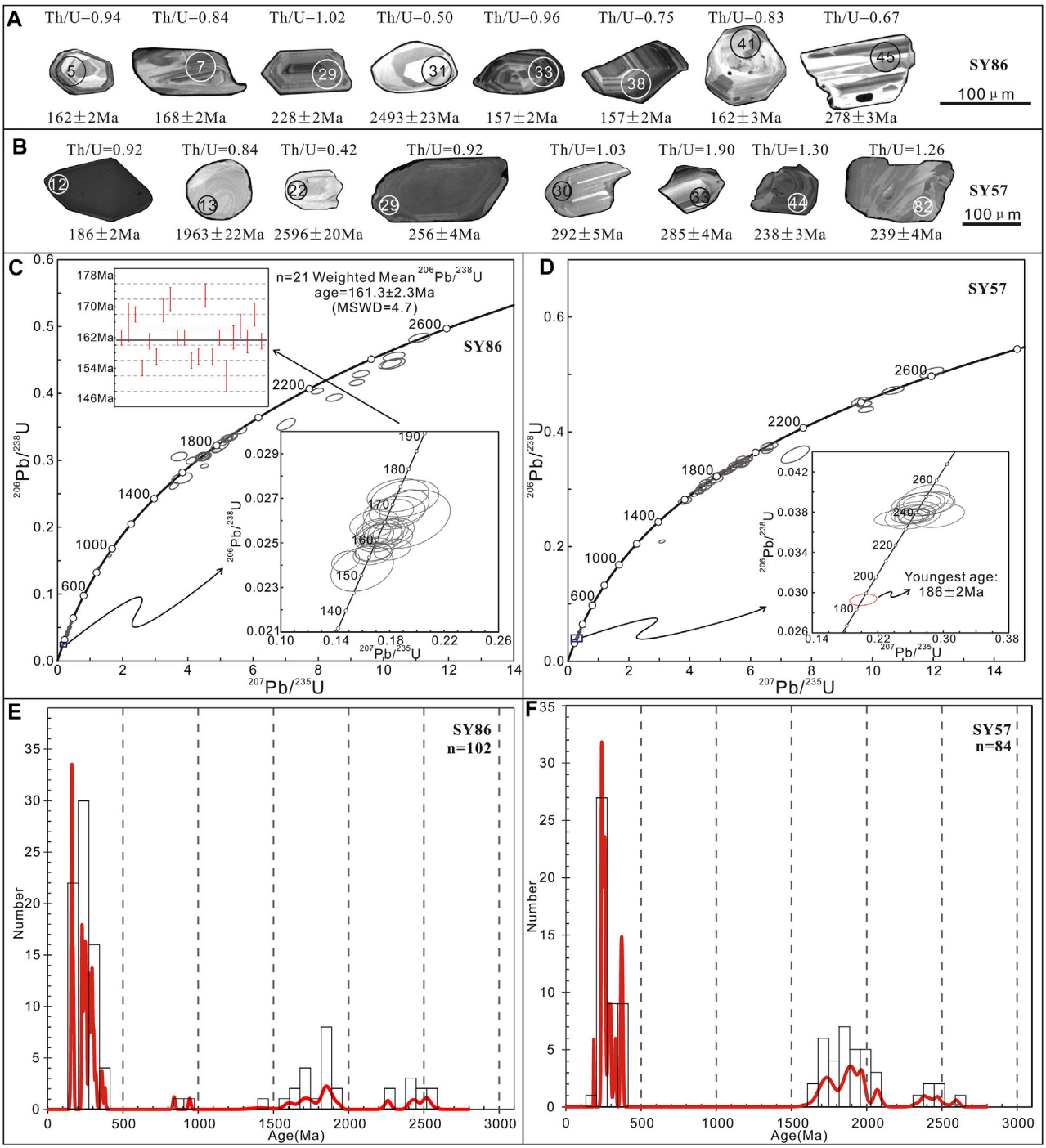

FIGURE 12 | Representative cathodoluminescence (CL) images of zircons and LA-ICP-MS U–Pb zircons dating results for samples SY86 and SY57. **(A,B)** CL images of zircons for samples SY86 and SY57, respectively. **(C,D)** Weighted mean calculations and concordia diagrams of zircon ages for samples SY86 and SY57, respectively. **(E,F)** Histograms of zircon ages for two samples (SY86 and SY57). *See* text for more details.

in **Figures 2A**, **11A,E**. The detailed results are presented in **Figure 12** and in the Appendix (**Supplementary Table A1**).

Sample SY86 was collected from a pyroclastic interlayer within the sandstones of the Jiulongshan Formation near the Beicaonian. This interlayer (10–15 m thick) is predominantly the andesitic volcanics mixed with bits of clastic deposit, and it's gently inclined to the northeast. Based on field observations, the apparent sedimentary contact between the andesitic pyroclastic rocks and the surrounding sandstone can be defined clearly (**Figures 11A,B**). The results show that apparent ages of 102 zircon grains are between 2533 ± 23 Ma and

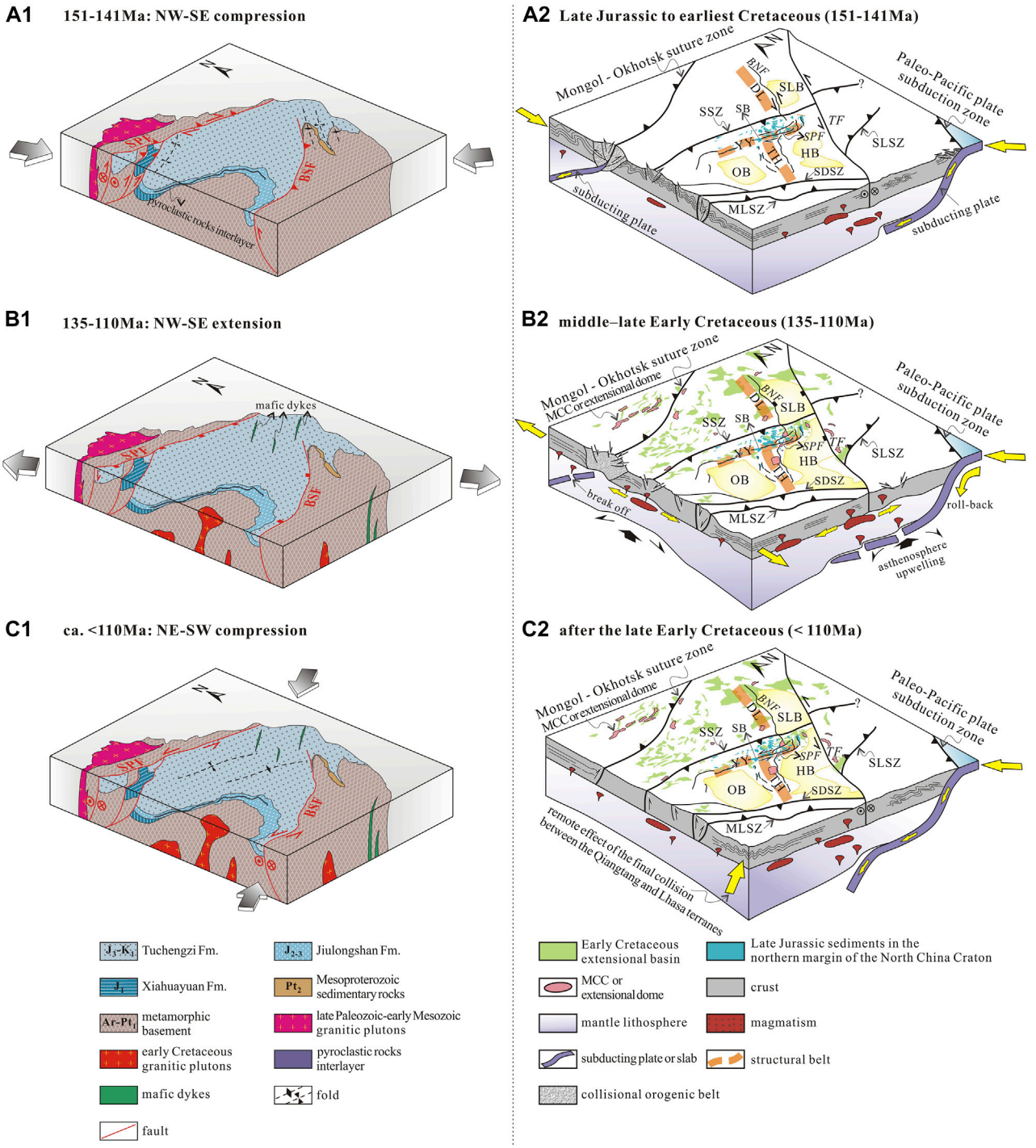

FIGURE 13 | Late Mesozoic tectonic evolution of the Shangyi area **(A1–C1)** and possible dynamic mechanisms **(A2–C2)** (modified after Wang et al., 2011; Wang et al., 2017). SLB, Songliao Basin; HB, Huabei Basin; OB, Ordos Basin; SSZ, Solonker-Linxi suture zone; SLSZ, Sulu suture zone; SDSZ, Shangdan suture zone; MLSZ, Mianlue suture zone. The rest figure captions are the same as **Figures 1A,B**. *See* text for more details.

152 ± 4 Ma (**Figures 12C,E**), with the younger ages (n = 21) defining a weighted mean $^{206}Pb/^{238}U$ age of 161.3 ± 2.3 Ma (MSWD = 4.7) (**Figure 12C**). These younger zircon grains are mostly subhedral, and a magmatic origin of them is inferred based on the recognition of oscillatory zoning in CL images (**Figure 12A**) and the Th/U ratios (0.54–1.26; **Supplementary Table A1**) (Belousova et al., 2002). The weighted mean $^{206}Pb/^{238}U$ age is interpreted as the formation age of the andesitic pyroclastic rocks, and also reflecting the formation age of the Jiulongshan Formation. Other older ages are possibly the detrital zircon ages (**Figures 12A,C,E**).

Sample SY57 was acquired from a NE-trending mafic dike intruded into the sandstones (Tuchengzi Formation) at the north of Jiashihe (**Figures 2A**, **11E,F**). This mafic dike, over 1 km in length and 1–2 m in width, may belong to the product of regional NW-SE extensional deformation. We intended to take the formation age of the dike to constrain the timing of NW-SE extension. Unfortunately, it did not work. Apparent ages of zircons (n = 84) are between 2596 ± 20 Ma and 186 ± 2 Ma (**Figures 12B,D,F** and **Supplementary Table A1**). The youngest age of 186 ± 2 Ma represents the Early Jurassic, which is overtly earlier than the age of surrounding Tuchengzi Formation and also precede the formation age of 161 Ma obtained from the Jiulongshan Formation. In consequence, all the ages may reflect the ages of the captured detrital zircons from the wall rocks rather than indicate the formation age of this mafic dike.

DISCUSSIONS AND INTERPRETATIONS

Timing of Three-phase Deformation

According to the analysis of multi-stage deformation, we established a relative evolutionary sequence of the basin during the late Mesozoic, including the early NW-SE compression, the middle NW-SE extension and the later NE-SW compression. The present bulk architecture of the basin was controlled by the early NW-SE compressional stress, and the subsequent two tectonic events only caused limited destruction to the previous tectonic framework.

Some fault striations associated with NW-SE compression and the X-type conjugate shear fractures resulted from NE-SW compression were simultaneously observed in the pyroclastic interlayer at the location of sample SY86 (**Figures 11B–D**), indicating that both of the two compressional events commenced posterior to 161 Ma. Our structural analysis has revealed that the Tuchengzi Formation is the youngest strata suffered from NW-SE compressional deformation. Many investigations suggest that the Tuchengzi Formation in the Yanshan belt is commonly marked by the molasse-like formations or synorogenic deposits (Zhao, 1990; Zhang, 1999; He et al., 2008), whose lower limit age has been usually constrained to 157–151 Ma (Cope, 2003; Xu et al., 2012; Qi et al., 2015; Fu et al., 2018). Furthermore, despite we failed to define the emplacement age of the NE-oriented mafic dike at the east edge of the basin from our sample SY57, Xu et al. (2016) reported a SHRIMP zircon U–Pb age of 141 ± 1 Ma from the mafic dikes that intrude in the upper part of the Tuchengzi Formation in the eastern Shangyi basin. Many other mafic dikes intruded in the Tuchengzi Formation were widely recognized in North China and Northeast China. Their ages of emplacement are concentrated in 144–140 Ma, indicating a regional extensional tectonic setting during the Early Cretaceous (Xu et al., 2017). Based on the analysis above, the timing of NW-SE compressional deformation can therefore be constrained to ca. 151–141 Ma. In the light of regional tectonic evolution, NW-SE compressional deformation was closely related to the episode B of the Yanshanian movement (Yanshanian B) in the NCC, expressed by territorial Late Jurassic–Early Cretaceous disconformities, series of fold-thrust structures and transpressional fault systems (Wong, 1927; Davis et al., 1998; Zhao et al., 2004; Zhang and Dong, 2008; Li et al., 2016; Zhu et al., 2018; Lin et al., 2019), which has been constrained to 160–135 Ma (Zhao et al., 2004; Zhu et al., 2015; Clinkscales and Kapp, 2019; Lin et al., 2019).

Niu et al. (2003) used the SHRIMP zircons U-Pb dating from the base of the Zhangjiakou Formation volcanics in the basin of the central Yanshan belt to determine the change in regional tectonic regime from compression to extension occurred at 136 Ma. As is well-known, during the Early Cretaceous, regional NW-SE extension was matched with widespread lithospheric extension and destruction in eastern China, manifested by massive magmatism and remarkable NE-trending basin-range structures, which has been normally constrained to 135–110 Ma (Wu et al., 2005; Wang et al., 2012, 2015; Daoudene et al., 2013; Zhu et al., 2018). The Early Cretaceous volcanics are absent in the Shangyi Basin. Whereas, Zhang (2019) recently provided new evidence of the magmatic activity in Shangyi area during the middle–late Early Cretaceous based on the zircons U–Pb ages of 135–123 Ma from the Huangyuwa granitic pluton (or the Xiaodaqingshan granites) at the northeast of Xinghe (**Figure 2A**). The above descriptions allows us to constrain the timing of NW-SE extension to ca. 135–110 Ma.

In the northern margin of North China, correlational studies of NE-SW compression during the late Mesozoic were rarely reported. Based on the comprehensive analysis of the intracontinental transform structures in the joint part of the Yanshan and Taihang Mountain belts during the Early Cretaceous, Lin et al. (2020) suggested that the Yanshan belt was marked by ~E-W-oriented sinistral extension after 129 Ma. A local NE-SW compressive stress field may be derived from this sinistral transtensional structure, whereas the multi-stage tectonic evolution sequences established in this paper cannot support this pattern. Actually, C. H. Zhang et al. (2004) investigated the NW-striking Taiying-Lengkou-Shangying Fault Zone in the central part of the Yanshan belt, which has experienced multi-phase tectonic movements in the late Mesozoic, including thrusting, extension and strike-slip faulting. A significant reversal faulting with the top-to-the-SW slip sense along the Taiying-Lengkou-Shangying Fault Zone occurred after the generated age of the late Early Cretaceous Jiufotang Formation, causing an asymmetric syncline with the NE-dipping axial plane was formed in the Jiufotang Formation in the footwall (C. H. Zhang et al., 2004). Moreover, Yang (2015) conducted the analysis of Mesozoic tectonic deformation and palaeostress field in the southern area of Jianchang, Western Liaoning Province, China and established a model of four-phase tectonic evolution. The NW- to NNW-oriented fold and fault system was considered as the result of the latest NE-SW compression, whose activity age was identified as later than the Jiufotang Formation (Yang, 2015). The Jiufotang Formation in the northern NCC is predominantly a set of fossil-bearing lacustrine sediments, whose age constraints was still lacking in reliable geochronology data and was generally defined by the research of Paleontology and Stratigraphy. He et al. (2004) reported the K-feldspars $^{40}Ar/^{39}Ar$ date of 120.3 ± 0.7 Ma from the tuff interlayer within the shale of the Jiufotang Formation at the Shangheshou section in Chaoyang, Liaoning, northeastern China. Another radioisotopic age of the Jiufotang Formation has been dated from Tebch, Inner Mongolia, with a $^{40}Ar/^{39}Ar$ age of 110.59 ± 0.52 Ma got from intrusive basalt within the Jiufotang Formation (Eberth et al., 1993), which may provide a

top limit for the Jiufotang Formation. In consequence, NE-SW compression may commence posterior to 110 Ma. Given that the Cenozoic strata in the study area were not involved in NE-SW compressional deformation, this tectonic event may occur at the late Early Cretaceous–Late Cretaceous.

Tectonic Origin of the Tuchengzi Formation

In addition to the Shangyi Basin, the Tuchengzi Formation is also extensively exposed in other typical late Mesozoic basins in the northern margin of the NCC. The origin of the Tuchengzi Formation was variously interpreted to be related to *1*) the flexural basin controlled by compression and thrusting (He et al., 2008; J. Liu et al., 2015; Liu et al., 2018; Lin et al., 2019); or *2*) intraplate rift environment (Shao et al., 2003; P. Zhang et al., 2014; Y. Q. Liu et al., 2015; Xu et al., 2016). According to this study, integrated with previous achievements, we believe that the Tuchengzi Formation of the Shangyi Basin developed during a compression environment. The reasons are as follows. *1*) Abundant chronological data show that the Tuchengzi Formation was formed in the Late Jurassic-Early Cretaceous (157–137 Ma) (Cope, 2003; Zhang et al., 2009 ; ; Xu et al., 2012; Wang et al., 2013; Qi et al., 2015; Li et al., 2016; Fu et al., 2018; Lin et al., 2019; Shi et al., 2019), which is consistent in time with the Yanshanian B. *2*) Since the lack of accurate chronological data, P. Zhang et al. (2014) and Xu et al. (2016) assigned the pyroclastic interlayer within the sandstones near the west edge of the basin to the Tuchengzi Formation, and they considered the pyroclastic deposit reflected an extensional environment during the depositional stage of the Tuchengzi Formation. However, our chronological results confirmed this set of pyroclastic rocks was formed at 161 Ma (**Figures 3**, **12C**), corresponding to the sedimentation time of 164–158 Ma from the lower part of the Jiulongshan Formation (Chen et al., 2014; Li et al., 2014; Lin, 2019). Meanwhile, numerous studies have shown that the molasse-like characteristics of the Tuchengzi Formation represent the thrust faulting from the basin-controlling faults (J. Liu et al., 2015; Liu et al., 2018; Lin et al., 2019, Shi et al., 2019). *3*) The overall tectonic framework of the basin is controlled by NW-SE compressional stress, and the synsedimentary normal faults associated with the Tuchengzi Formation are not found on the edges of the basin (He et al., 2008). Xu et al. (2016) took the Early Cretaceous mafic dikes intrude in the upper part of the Tuchengzi Formation in the Shangyi basin as the result of syntectonic emplacement during the late sedimentary stage of this formation, suggesting an extensional tectonic setting. Nevertheless, based on our fieldwork, these mafic dikes are not appeared as the interlayers but manifested as evident cross-cutting relationships with the surrounding strata (**Figures 11E,F**), which implies that the regional extension may later than the Tuchengzi Formation. *4*) The stratigraphic succession of the Tuchengzi Formation in Shangyi area is characterized by an upward decrease in grain size (**Figure 3**), which is inconsistent in sedimentary characteristics with that in others Mesozoic basins (such as the Luanping Basin, the Chicheng Basin, and the Qianjiadian Baisn) in the Yanshan belt, expressed by a sequence with fining-upward first and then coarsening-upward in grain size (J. Liu et al., 2015; Lin et al., 2019; Shi et al., 2019). This difference may be related to the geotectonic location of the study area. Related research reveals that the Taihang Mountains might have experienced two significant tectonic uplifts during the late Middle Jurassic to Early Cretaceous (Wang and Li, 2008; Cao et al., 2013; Yang et al., 2014), which may result in the denudation of the upper part of the Tuchengzi Formation and the lack of late Mesozoic volcanic rocks in Shangyi region.

Of course, we are not ruling out that some transitory tectonic quiet periods (even the short-lived weak extensional episodes) may occur in the depositional phase of the Tuchengzi Formation. Shi et al. (2019) confirmed that the middle and upper part of the Tuchengzi Formation in the Qianjiadian Basin in the western Yanshan fold and thrust belt was controlled by the NE-striking Qianjiadian thrust fault and the SPF. Before that, the basin has experienced an obvious lake transgression event during the early deposition of the Tuchengzi Formation, suggesting a temporary tectonic quiet period (Shi et al., 2019).

Implications of Crustal Shortening-thickening to Craton Destruction

Based on restoration of the section B-B', we obtained the minimum crustal shortening ratio of 27% in Shangyi area under the control of NW-SE compression during the late Late Jurassic to earliest Cretaceous. Horizontal shortening of the crust was principally accommodated by vertical crust thickening resulted from the thrust faulting and the buckle folding. Numerous studies confirmed that the Yanshanian movement caused conspicuous thickening of the lithosphere in eastern China during the late Mesozoic (Zhao et al., 2004; Zhang et al., 2008; Dong et al., 2015, 2018). Based on balanced cross-section reconstructions, Zhang et al. (2011) estimated the north-south-directed shortening of the central part of the Yanshan belt before 135 Ma was around 38%, causing crustal thickening up to 12–15 km. Subsequently, the tectonic regime in eastern China and its adjacent areas underwent a remarkable transition from compression to extension, generating extensive lithospheric destruction and thinning. In recent years, some significant evidence of early crustal shortening-thickening has been discovered from some representative low-angle detachment systems or metamorphic core complexes developed in the northern margin of the NCC (Wang et al., 2011; Zhu et al., 2015), indicating an intimate relationship between crustal shortening-thickening and lithospheric destruction. On the one hand, the thickened crust may usually give rise to deep-seated partial melting, and then continuous melting may cause the weakening of deep-seated rocks and may further trigger crust–mantle decoupling (Liu et al., 2009, 2020). On the other hand, lithospheric isostasy and the coeval magmatism caused the thickened crust uplifted significantly accompanied with increasing gravitational potential energy, which incurred the destruction of the original stability of the craton and also provided favorable conditions for the subsequent intense extensional collapse of the middle and upper crust (Zheng and Wang, 2005; Wang et al., 2011; Zhang et al., 2011).

Tectonic Evolution and Geodynamic Interpretation

Intracontinental deformation events occurred at pre-Late Jurassic in the north edge of the NCC had been recognized in many studies.

For instance, some significant ~E-W-striking faults in Yanshan belt, including the Fengning-Longhua Fault, the Gubeikou-Pingquan Fault (namely the eastern the Shangyi-Pingquan Fault) (**Figure 1B**) and so on, were characterized by thrusting towards the south of hanging wall during the pre-Middle Jurassic (J. Liu et al., 2012; Li et al., 2016; S. F. Liu et al., 2021), indicating the ~N-S crustal shortening. Afterwards, a regional unconformity interface formed between the Tiaojishan Formation and the underlying older stratigraphic units, which reflects the episode A of the Yanshanian movement. Furthermore, a set of molasse-like formations represented by the Longmen Formation conglomerates from the Western Hills of Beijing acted as the crucial sedimentary response of this tectonic movement (Xu et al., 2016). However, in view of limited structural data in this work, here we mainly discuss the Late Jurassic-Cretaceous tectonic deformation in the northern margin of North China.

During the Late Jurassic to earliest Cretaceous (ca. 151–141 Ma), after the short tectonic quiet period, another intense intracontinental deformation event, namely the episode B of the Yanshanian movement, occurred in northern margin of the NCC. The SPF, as the north boundary of the Shangyi Basin, reactivated under the influence of regional NW-SE compression, expressed by obvious dextral strike-slip movement. Meanwhile, the BSF was formed on the southern edge of the basin and was marked by a reverse fault with the top-to-the-NW slip sense. These thrust structures have shown as the basement-involved thick-skinned tectonics, which made all the late Mesozoic strata in the basin subject to folding and thrusting and formed a structural style of facing thrusts (**Figure 13A1**). In addition, some evidence related to the ~N-S contraction deformation has also been identified simultaneously in the north margin of the NCC. For example, Zhu et al. (2015) reported that the Sihetang ductile shear zone in the middle of the Yanshan belt was a thrusting zone with the top-to-the-SSW shear sense during the early Early Cretaceous (140–137 Ma); Davis et al. (2001) deemed that the high-angle Gubeikou Fault shown as a thrust fault with the top-to-the-south slip sense during the Late Jurassic to earliest Cretaceous (148–132 Ma). The above information demonstrates that the north edge of the North China might be affected by multiple tectonic domains in this period.

The geodynamics of NW-SE compression in this stage was normally considered as the subduction of the Paleo-Pacific plate beneath the East Asian continent (Liu et al., 2017, 2018; Zhu et al., 2018; Clinkscales and Kapp, 2019; Lin et al., 2019). However, this suggestion cannot explain the simultaneous ~N-S or NNE compressional deformation in the northern margin of the NCC (Lin et al., 2013), which was usually attributed to the closure of the Mongol-Okhosk Ocean (Zorin, 1999; Davis et al., 2001; Meng, 2003; Donskaya et al., 2008; Wang et al., 2011, 2015; Zhu et al., 2015). Some studies suggest that the Mongol-Okhotsk Ocean began to close from west to east in a scissor-like fashion during the late Mesozoic, and the final collision may occur in the Early Cretaceous (Metelkin et al., 2010). Under the influence of the closure of the Mongol-Okhosk Ocean in the north, series of N-S-directed tectonic shortening were marked in the northern margin of the NCC (He et al., 1998). Therefore, this stage of tectonic event (namely the Yanshanian B) may be driven by a combined effect from both of the subduction of the Paleo-Pacific plate beneath East Asia and the closure of the Mongol-Okhosk Ocean (**Figure 13A2**).

During the middle–late Early Cretaceous (ca. 135–110 Ma), the NCC underwent widespread lithospheric extension and destruction, expressed by vast magmatism and the development of abundant extensional structures. Due to previous compression and uplifting, the Early Cretaceous volcanics are quite undeveloped in Shangyi area. Nevertheless, under the control of regional NW-SE extension, some outcrop-scale extensional structures were formed in margins and interior of the basin, and some coeval mafic dikes and intermediate-acid granites were also invaded sporadically in the east and west sides (**Figure 13B1**). Compared with the contemporaneous representative extensional basins and low-angle detachment systems (or metamorphic core complexes) in the northern margin of the NCC (Wang et al., 2011, 2012; Lin and Wei, 2018), the strength and influence of NW-SE extensional deformation in the Shangyi Basin are very limited and are not change the previous tectonic framework, which may reflect the inhomogeneous extension and thinning of the lithosphere (Xu, 2004; Liu et al., 2009). Many researchers linked far-ranging NW–SE extensional deformation in North China during the Early Cretaceous to the roll-back of the Paleo-Pacific subducting plate (Griffin et al., 1998; Davis et al., 2001; Ren et al., 2002; Zhu et al., 2011; Liu et al., 2017; B. Zhang et al., 2020). However, many extensional structures, such as half-graben basins, metamorphic core complexes, and syntectonic plutons bounded by low-angle normal faults, were also recognized in Transbaikalia and adjacent areas in the northern Central Asian Orogenic Belt, whose origin was owed to post-orogenic extensional collapse of the Mongol–Okhotsk belt (Zorin, 1999; Meng, 2003; Donskaya et al., 2008; Wang et al., 2011). These extensional structures show the highly consistent in activity age with the lithospheric extension and thinning of the NCC (Donskaya et al., 2008; Wang et al., 2012, 2015; Daoudene et al., 2013; Lin and Wei, 2018). Furthermore, in terms of the geotectonic position, the distance between the northern margin of the NCC and the subducting edge in the east is roughly the same as the distance from the northern margin of the NCC to the Mongol–Okhotsk belt in the north (**Figure 1A**). The geodynamic context of this far-ranging NW–SE extensional event is thus likely associated with back-arc extension triggered by the roll-back of the Paleo-Pacific subducting plate and post-orogenic extensional collapse of the Mongol–Okhotsk belt (**Figure 13B2**).

After the late Early Cretaceous (<110 Ma) (or may be during the late Early Cretaceous–Late Cretaceous), the Shangyi Basin experienced NE-SW compression. This compressional event, whereas, only caused limited destruction and transformation to the early structures, which was shown as local strike-slip displacement along the boundary faults, some outcrop-scale X-type conjugate shear fractures, and NW-trending open fold (**Figure 13C1**). It should be noted that the Cretaceous faulted basin in Eastern China experienced an important tectonic reverse associated with another NW-SE compressive stress field during the late Early Cretaceous-Late Cretaceous (Y. Q. Zhang et al., 2004; Liu et al., 2017; B. Zhang et al., 2020), which reflects termination of the NCC peak destruction. Here NW-SE compression is inconsistent in orientation with the

contemporaneous NE-SW compression, implying a complex tectonic situation of intracontinental multidirectional compressional deformation in the north edge of the NCC during this period.

About the driving mechanism, on the one hand, this stage of NW-SE compression may be linked to the change of velocity and angle of the subducting plate (Zhang et al., 2008; Zhu et al., 2018; B. Zhang et al., 2020). After further analysis, some researchers have argued that an undefined ocean block or plateau collided with the southeast margin of East Asia continent during the Late Cretaceous (ca. 100 Ma) (Yang, 2013; Niu et al., 2015; J. Zhang et al., 2020). Then this unknown block continued moving to the north along the east margin of East Asia, which affected the compression-shear structural environment in the east edge of East Asia. In this process, Paleo-Pacific Plate changed into low-angle subduction again (**Figure 13C2**) (Yang, 2013; J. Zhang et al., 2020). However, on the other hand, NE-SW compression is almost perpendicular in orientation to the subduction of the Paleo-Pacific plate, so the latter is unlikely to be the geodynamic background of the former. Simultaneously, the Mongol-Okhosk Ocean has closed, suggesting the driving force may not be from the north. Actually, the Qiangtang and Lhasa terranes at the southwest of the NCC (**Figure 1A**) experienced collision and collage during the Mesozoic (Guynn et al., 2006; Kapp et al., 2007; Ma et al., 2017). The Bangong-Nujiang suture zone, as the boundary between the Qiangtang and Lhasa terranes, represents the relic of the Mesozoic Bangong–Nujiang Tethyan Ocean (Wang et al., 2016). Recently, Peng et al. (2020) conducted a systematic petrologic, geochemical and isotope chronological investigation in Tongka area, which is located in the eastern section of the Bangong-Nujiang suture. They deemed that the initial subduction of the Bangong–Nujiang Tethyan Ocean may start at 190 Ma, and its eventual closure may continue to the Late Cretaceous (Peng et al., 2020). Considering that the subduction and closure of the Bangong–Nujiang Tethyan Ocean is consistent in direction with regional NE-SW compression, we can speculate that the NE-SW compression may be linked to the remote effect of the final collision between the Qiangtang and Lhasa terranes (**Figure 13C2**).

CONCLUSION

According to our results, the following conclusions can be drawn.

(1) We delineate three phases of intracontinental deformation in the Shangyi Basin during the late Mesozoic in the following chronological order: NW-SE compression during the Late Jurassic to earliest Cretaceous (ca. 151–141 Ma); NW-SE extension during the middle–late Early Cretaceous (ca. 135–110 Ma); and NE-SW compressional deformation later than 110 Ma. NW-SE compression controlled the present basic tectonic framework of the basin, and the subsequent two tectonic deformations only caused limited destruction to the previous structures.
(2) Based on balanced cross-section restoration, we estimate the minimum crustal shortening ratio of 27% in Shangyi area under the control of NW-SE compression. Moreover, the contribution of tectonic shortening from the north side of the basin is greater than that from the south side.
(3) NW-SE compression is consistent in activity age with the episode B of the Yanshanian movement, and the latter may be related to the subduction of the Paleo-Pacific plate beneath East Asia and the closure of the Mongol-Okhosk Ocean. The subsequent NW–SE extensional event is likely to be reflects the destruction of the NCC during the Early Cretaceous, which may result from the roll-back of the Paleo-Pacific plate and post-orogenic extensional collapse of the Mongol-Okhotsk belt. The NE-SW compressional deformation may be related to the remote effect of the final collision between the Qiangtang and Lhasa terranes.

DATA AVAILABILITY STATEMENT

The original contributions presented in the study are included in the article/**Supplementary Material**, further inquiries can be directed to the corresponding authors.

ETHICS STATEMENT

Written informed consent was obtained from the individual(s) for the publication of any potentially identifiable images or data included in this article.

AUTHOR CONTRIBUTIONS

QY: Data curation, Methodology, Investigation, Formal analysis, Writing- Original draft preparation, Visualization. WS: Conceptualization, Methodology, Investigation, Writing - Review & Editing, Supervision, Project administration, Funding acquisition. GH: Conceptualization, Validation, Writing - Review & Editing, Supervision. YZ: Software, Formal analysis, Investigation. YZ: Investigation.

FUNDING

This study is supported by the National Key R&D Plan of Ministry of Science and Technology of China (Grant No. 2017YFC0601402) and the General Project of National Natural Science Foundation of China (Grant No. 41672203). We are grateful to the editors and reviewers for their critical and constructive comments to improve the manuscript.

SUPPLEMENTARY MATERIAL

The Supplementary Material for this article can be found online at: https://www.frontiersin.org/articles/10.3389/feart.2021.710758/full#supplementary-material

REFERENCES

Allmendinger, R. W., Cardozo, N., and Fisher, D. M. (2012). *Structural Geology Algorithms: Vectors and Tensors*. New York, NY: Cambridge University Press, 1–289.

Angelier, J. (1979). Determination of the Mean Principal Directions of Stresses for a Given Fault Population. *Tectonophysics* 56 (3–4), T17–T26. doi:10.1016/0040-1951(79)90081-7

Angelier, J. (1984). Tectonic Analysis of Fault Slip Data Sets. *J. Geophys. Res.* 89 (B7), 5835–5848. doi:10.1029/JB089iB07p05835

Belousova, E., Griffin, W., O'Reilly, S. Y., and Fisher, N. (2002). Igneous Zircon: Trace Element Composition as an Indicator of Source Rock Type. *Contrib. Mineral. Petrol.* 143 (5), 602–622. doi:10.1007/s00410-002-0364-7

Bott, M. H. P. (1959). The Mechanics of Oblique Slip Faulting. *Geol. Mag.* 96, 109–117. doi:10.1017/S0016756800059987

Cao, X. Z., Li, S. Z., Liu, X., Suo, Y. H., Zhao, S. J., Xu, L. Q., et al. (2013). The Intraplate Morphotectonic Inversion Along the Eastern Taihang Mountain Fault Zone, North China and its Mechanism. *Earth Sci. Frontiersn* 20 (4), 88–103. (in Chinese).

Chang, S.-C., Zhang, H., Hemming, S. R., Mesko, G. T., and Fang, Y. (2013). ^{40}Ar/^{39}Ar Age Constraints on the Haifanggou and Lanqi Formations: When Did the First Flowers Bloom? *Geol. Soc. Lond. Spec. Publications* 378, 277–284. doi:10.1144/sp378.1

Chang, S.-c., Zhang, H., Renne, P. R., and Fang, Y. (2009). High-precision ^{40}Ar/^{39}Ar Age Constraints on the Basal Lanqi Formation and its Implications for the Origin of Angiosperm Plants. *Earth Planet. Sci. Lett.* 279 (3-4), 212–221. doi:10.1016/j.epsl.2008.12.045

Chen, H. Y., Zhang, Y. Q., Zhang, J. D., Fan, Y. G., Peng, Q. P., Lian, Q., et al. (2014). LA-ICP-MS Zircon U-Pb Age and Geochemical Characteristics of Tuff of Jiulongshan Formation from Chengde Basin, Northern Hebei. *Geol. Bull. China* 33 (7), 966–973. (in Chinese).

Chen, P., and Shi, W. (2015). Theory and Practice of Paleostress Field Inversion: Inferred from Fault Slip Vector Analysis. *Geol. Rev.* 61 (3), 536–546. (in Chinese).

Clinkscales, C., and Kapp, P. (2019). Structural Style and Kinematics of the Taihang-Luliangshan Fold belt, North China: Implications for the Yanshanian Orogeny. *Lithosphere* 11 (6), 767–783. doi:10.1130/L1096.1

Cope, T. D. (2003). *Sedimentary Evolution of the Yanshan Fold-Thrust Belt, Northeast China*. Stanford, CA: Stanford University, 1–230.

Cope, T. D., Shultz, M. R., and Graham, S. A. (2007). Detrital Record of Mesozoic Shortening in the Yanshan Belt, NE China: Testing Structural Interpretations with basin Analysis. *Basin Res.* 19 (2), 253–272. doi:10.1111/j.1365-2117.2007.00321.x

Cui, S. Q., and Wu, Z. H. (2002). "On the Mesozoic and Cenozoic Intracontinental Orogenises of Yanshan Area," in *Orogenic Process and Dynamic Mechanism of the Yanshan Intracontinental Orogenic Belt*. Editors S. Q. Cui, Y. S. Ma, and Z. H. Wu (Beijing: Geology Publishing House), 56–61.

Dahlstrom, C. D. A. (1969). Balanced Cross Sections. *Can. J. Earth Sci.* 6, 743–757. doi:10.1139/e69-069

Dai, L.-Q., Zheng, Y.-F., and Zhao, Z.-F. (2016). Termination Time of Peak Decratonization in North China: Geochemical Evidence from Mafic Igneous Rocks. *Lithos* 240-243, 327–336. doi:10.1016/j.lithos.2015.11.014

Daoudene, Y., Ruffet, G., Cocherie, A., Ledru, P., and Gapais, D. (2013). Timing of Exhumation of the Ereendavaa Metamorphic Core Complex (North-eastern Mongolia) - U-Pb and ^{40}Ar/^{39}Ar Constraints. *J. Asian Earth Sci.* 62, 98–116. doi:10.1016/j.jseaes.2011.04.009

Davis, G. A., Wang, C., Zheng, Y., Zhang, J., Zhang, C., and Gehrels, G. E. (1998). The Enigmatic Yinshan Fold-And-Thrust Belt of Northern China: New Views on its Intraplate Contractional Styles. *Geology* 26, 43–46. doi:10.1130/0091-7613(1998)026<0043:TEYFAT>2.3.CO;2

Davis, G. A., Zheng, Y. D., Wang, C., Darby, B. J., Zhang, C. H., and Gehrels, G. E., (2001). Mesozoic Tectonic Evolution of the Yanshan Fold and Thrust Belt, with Emphasis on Hebei and Liaoning Provinces, Northern China. *Memoir Geol. Soc. America* 194, 171–197. doi:10.1130/0-8137-1194-0.171

Delvaux, D., Moeys, R., Stapel, G., Melnikov, A., and Ermikov, V. (1995). Palaeostress Reconstructions and Geodynamics of the Baikal Region, Central Asia, Part I. Palaeozoic and Mesozoic Pre-rift Evolution. *Tectonophysics* 252 (1), 61–101. doi:10.1016/0040-1951(95)00090-9

Delvaux, D., and Sperner, B. (2003). New Aspects of Tectonic Stress Inversion with Reference to the TENSOR Program. *Geol. Soc. Lond. Spec. Publications* 212 (1), 75–100. doi:10.1144/GSL.SP.2003.212.01.06

Dong, C., Wan, Y., Xu, Z., Liu, D., Yang, Z., Ma, M., et al. (2013). SHRIMP Zircon U-Pb Dating of Late Paleoproterozoic Kondalites in the Daqing Mountains Area on the North China Craton. *Sci. China Earth Sci.* 56 (1), 115–125. doi:10.1007/s11430-012-4459-3

Dong, S. W., Zhang, Y. Q., Long, C. X., Yang, Z. Y., Ji, Q., Wang, T., et al. (2007). Jurassic Tectonic Revolution in China and New Interpretation of the Yanshan Movement. *Acta Geologica Sinica* 81 (11), 1449–1461. (in Chinese).

Dong, S., Zhang, Y., Li, H., Shi, W., Xue, H., Li, J., et al. (2018). The Yanshan Orogeny and Late Mesozoic Multi-Plate Convergence in East Asia-Commemorating 90th Years of the "Yanshan Orogeny". *Sci. China Earth Sci.* 61 (12), 1888–1909. doi:10.1007/s11430-017-9297-y

Dong, S., Zhang, Y., Zhang, F., Cui, J., Chen, X., Zhang, S., et al. (2015). Late Jurassic-Early Cretaceous continental Convergence and Intracontinental Orogenesis in East Asia: A Synthesis of the Yanshan Revolution. *J. Asian Earth Sci.* 114, 750–770. doi:10.1016/j.jseaes.2015.08.011

Dong, Y., Zhang, G., Neubauer, F., Liu, X., Genser, J., and Hauzenberger, C. (2011). Tectonic Evolution of the Qinling Orogen, China: Review and Synthesis. *J. Asian Earth Sci.* 41 (3), 213–237. doi:10.1016/j.jseaes.2011.03.002

Donskaya, T. V., Windley, B. F., Mazukabzov, A. M., KRöNER, A., Sklyarov, E. V., Gladkochub, D. P., et al. (2008). Age and Evolution of Late Mesozoic Metamorphic Core Complexes in Southern Siberia and Northern Mongolia. *J. Geol. Soc.* 165 (1), 405–421. doi:10.1144/0016-76492006-162

Eberth, D. A., Russell, D. A., Braman, D. R., and Deino, A. L. (1993). The Age of the Dinosaur-bearing Sediments at Tebch, Inner Mongolia, People's Republic of China. *Can. J. Earth Sci.* 30 (10), 2101–2106. doi:10.1139/e93-182

Eizenhöfer, P. R., Zhao, G., Zhang, J., and Sun, M. (2014). Final Closure of the Paleo-Asian Ocean along the Solonker Suture Zone: Constraints from Geochronological and Geochemical Data of Permian Volcanic and Sedimentary Rocks. *Tectonics* 33 (4), 441–463. doi:10.1002/2013TC003357

Etchecopar, A., Vasseur, G., and Daignieres, M. (1981). An Inverse Problem in Microtectonics for the Determination of Stress Tensors from Fault Striation Analysis. *J. Struct. Geology.* 3 (1), 51–65. doi:10.1016/0191-8141(81)90056-0

Fu, Z.-B., Zhao, Y., Liu, J.-L., Zhang, S.-H., and Gao, H.-L. (2018). Revisiting of the Yanshanian Basins in Western and Northern Beijing, North China. *J. Asian Earth Sci.* 163, 90–107. doi:10.1016/j.jseaes.2018.05.016

Graham, S. A., Hendrix, M. S., Johnson, C. L., Badamgarav, D., Badarch, G., Amory, J., et al. (2001). Sedimentary Record and Tectonic Implications of Mesozoic Rifting in Southeast Mongolia. *Geol. Soc. America Bull.* 113, 1560–1579. doi:10.1130/0016-7606(2001)113<1560:SRATIO>2.0.CO;2

Griffin, W. L., Andi, Z., O'Reilly, S. Y., and Ryan, C. G. (1998). "Phanerozoic Evolution of the Lithosphere Beneath the Sino-Korean Craton," in *Mantle Dynamics and Plate Interactions in East Asia*. Editors M. F. J. Flower, S. L. Chung, and C. H. Lo (Washington, DC: Amer Geophysical Union), 27, 107–126. doi:10.1029/gd027p0107

Guynn, J. H., Kapp, P., Pullen, A., Heizler, M., Gehrels, G., and Ding, L. (2006). Tibetan Basement Rocks Near Amdo Reveal "Missing" Mesozoic Tectonism Along the Bangong Suture, Central Tibet. *Geol.* 34 (6), 505–508. doi:10.1130/G22453.1

Hao, W., Zhu, R., and Zhu, G. (2021). Jurassic Tectonics of the Eastern North China Craton: Response to Initial Subduction of the Paleo-Pacific Plate. *GSA Bull.* 133 (1-2), 19–36. doi:10.1130/B35585.1

He, H. Y., Wang, X. L., Zhou, Z. H., Wang, F., Boven, A., Shi, G. H., et al. (2004). Timing of the Jiufotang Formation (Jehol Group) in Liaoning, Northeastern China, and its Implications. *Geophys. Res. Lett.* 31 (12), L12605. doi:10.1029/2004GL019790

He, Z. J., Li, J. Y., Niu, B. G., and Ren, J. S. (1998). A Late Jurassic Intense Thrusting-Uplifting Event in the Yanshan–Yinshan Area, Northern China, and its Sedimentary Response. *Geol. Rev.* 44, 407–418. (in Chinese).

He, Z. J., Niu, B. G., and Zhang, X. Y. (2008). Sedimentary Response of the Shangyi basin, Northwestern Hebei, to the Late Jurassic Tectonism. *Geology. China* 35, 181–195. (in Chinese).

Hossack, J. R. (1979). The Use of Balanced Cross-Sections in the Calculation of Orogenic Contraction: A Review. *J. Geol. Soc.* 136 (6), 705–711. doi:10.1144/gsjgs.136.6.0705

Hou, G., Wang, Y., and Hari, K. R. (2010). The Late Triassic and Late Jurassic Stress fields and Tectonic Transmission of North China Craton. *J. Geodynamics* 50, 318–324. doi:10.1016/j.jog.2009.11.007

Hu, L., and Song, H. L. (2002). Ages of Activities of Southern "Inner Mongolia axis" Marginal Fault Belt and an Analysis of its Structure. *Geology China* 29 (4), 369–373. (in Chinese).

Huang, D. (2019). Jurassic Integrative Stratigraphy and Timescale of China. *Sci. China Earth Sci.* 62 (1), 223–255. doi:10.1007/s11430-017-9268-7

Huang, X., Shi, W., Chen, P., and Li, H. (2015). Superposed Deformation in the Helanshan Structural Belt: Implications for Mesozoic Intracontinental Deformation of the North China Plate. *J. Asian Earth Sci.* 114, 140–154. doi:10.1016/j.jseaes.2015.05.027

Kapp, P., DeCelles, P. G., Gehrels, G. E., Heizler, M., and Ding, L. (2007). Geological Records of the Lhasa-Qiangtang and Indo-Asian Collisions in the Nima Area of Central Tibet. *Geol. Soc. America Bull.* 119 (7–8), 917–933. doi:10.1130/B26033.1

Lacombe, O. (2012). Do Fault Slip Data Inversions Actually Yield "Paleostresses" that Can Be Compared with Contemporary Stresses? A Critical Discussion. *Comptes Rendus Geosci.* 344 (3-4), 159–173. doi:10.1016/j.crte.2012.01.006

Li, C., Zhang, C., Cope, T. D., and Lin, Y. (2016). Out-of-sequence Thrusting in Polycyclic Thrust Belts: An Example from the Mesozoic Yanshan Belt, North China Craton. *Tectonics* 35 (9), 2082–2116. doi:10.1002/2016TC004187

Li, D., Jin, Y., Hou, K., Chen, Y., and Lu, Z. (2015). Late Paleozoic Final Closure of the Paleo-Asian Ocean in the Eastern Part of the Xing-Meng Orogenic Belt: Constrains from Carboniferous-Permian (Meta-) Sedimentary Strata and (Meta-) Igneous Rocks. *Tectonophysics* 665, 251–262. doi:10.1016/j.tecto.2015.10.007

Li, H. L., Zhang, H. R., Qu, H. J., Cai, X. M., and Wang, M. (2014). Initiation, the First Stage of the Yanshan (Yenshan) Movement in Western Hills, Constraints from Zircon U-Pb Dating. *Geol. Rev.* 60, 1026–1042. (in Chinese).

Li, J., and Hou, G. (2018). Cretaceous Stress Field Evolution and Origin of the Jiaolai Basin, Eastern North China. *J. Asian Earth Sci.* 160, 258–270. doi:10.1016/j.jseaes.2018.01.024

Li, S., and Wang, Y. (2018). Formation Time of the Big Mantle Wedge Beneath Eastern China and A New Lithospheric Thinning Mechanism of the North China Craton-Geodynamic Effects of Deep Recycled Carbon. *Sci. China Earth Sci.* 61 (7), 853–868. doi:10.1007/s11430-017-9217-7

Li, S., Zhao, G., Dai, L., Liu, X., Zhou, L., Santosh, M., et al. (2012). Mesozoic Basins in Eastern China and Their Bearing on the Deconstruction of the North China Craton. *J. Asian Earth Sci.* 47, 64–79. doi:10.1016/j.jseaes.2011.06.008

Li, W., Guo, T. T., Wu, Z. P., Xu, C. G., Wu, K., Chen, X. P., et al. (2019). Application of Balanced Cross-Section Method in Extension, Strike-Slip Superposition and Ratio Analysis: A Case Study of Liaodong Bay Depression, Bohai Bay Basin. *Geol. Rev.* 65 (6), 1501–1514. (in Chinese).

Li, Y., Wang, C., Ma, C., Xu, G., and Zhao, X. (2011). Balanced Cross-Section and Crustal Shortening Analysis in the Tanggula-Tuotuohe Area, Northern Tibet. *J. Earth Sci.* 22 (1), 1–10. doi:10.1007/s12583-011-0152-2

Lin, C. F. (2019). *Jurassic Tectono-Sedimentary Evolution History of the Western Yanshan Fold-Thrust Belt, North China, and its Tectonic Implication*. Beijing: PhD Thesis. China University of Geosciences, 1–203.

Lin, C., Liu, S., Shi, X., and Zhuang, Q. (2019). Late Jurassic-Early Cretaceous Deformation in the Western Yanshan Fold-Thrust Belt: Insights from Syntectonic Sedimentation in the Chicheng Basin, North China. *Tectonics* 38 (7), 2449–2476. doi:10.1029/2018TC005402

Lin, W., Faure, M., Chen, Y., Ji, W., Wang, F., Wu, L., et al. (2013). Late Mesozoic Compressional to Extensional Tectonics in the Yiwulüshan Massif, NE China and its Bearing on the Evolution of the Yinshan-Yanshan Orogenic Belt. *Gondwana Res.* 23 (1), 54–77. doi:10.1016/j.gr.2012.02.013

Lin, W., and Wei, W. (2018). Late Mesozoic Extensional Tectonics in the North China Craton and its Adjacent Regions: A Review and Synthesis. *Int. Geology. Rev.* 62, 811–839. doi:10.1080/00206814.2018.1477073

Lin, Y., Zhang, C. H., Li, C. M., and Shi, X. L. (2015). Paleotectonic Stress Field and its Evolution in Central Part of the Intraplate Yanshan Orogenic Belt during Middle Jurassic and Early Cretaceous: Constrains of Stress Inversion of Fault Slip Vectors. *Geotectonica et Metallogenia* 39 (2), 187–207. (in Chinese).

Lin, Y., Zhang, C., Li, C., and Deng, H. (2020). From Dextral Contraction to Sinistral Extension of Intracontinental Transform Structures in the Yanshan and Northern Taihang Mountain Belts during Early Cretaceous: Implications to the Destruction of the North China Craton. *J. Asian Earth Sci.* 189, 104139. doi:10.1016/j.jseaes.2019.104139

Liu, J., Davis, G. A., Ji, M., Guan, H., and Bai, X. (2008). Crustal Detachment and Destruction of the Keel of North China Craton: Constraints from Late Mesozoic Extensional Structures. *Earth Sci. Front.* 15 (3), 72–81. doi:10.1016/s1872-5791(08)60063-9

Liu, J. L., Ji, M., Xia, H. R., Liu, Z. H., Zhou, Y. S., Yu, X. Q., et al. (2009). Crustal-mantle Detachment of the North China Craton in Late Mesozoic: Rheological Constraints. *Acta Petrologica Sinica* 25 (8), 1819–1829. (in Chinese).

Liu, J. L., Ni, J. L., Chen, X. Y., Craddock, J. P., Zheng, Y. Y., Sun, Y. Q., et al. (2020). Parallel Extension Tectonics: Mechanism of Early Cretaceous Thinning and Destruction of the Lithosphere of the North China Craton. *Acta Petrologica Sinica* 36, 2331–2343. doi:10.18654/1000-0569/2020.08.04

Liu, J., Ni, J., Chen, X., Craddock, J. P., Zheng, Y., Ji, L., et al. (2021). Early Cretaceous Tectonics Across the North Pacific: New Insights from Multiphase Tectonic Extension in Eastern Eurasia. *Earth-Science Rev.* 217, 103552. doi:10.1016/j.earscirev.2021.103552

Liu, J., Zhao, Y., Liu, A., and Ye, H. (2015). Late Jurassic to Early Cretaceous Sedimentary-Tectonic Development in the Chengde Basin, Yanshan Fold-Thrust Belt, North China Craton. *J. Asian Earth Sci.* 114, 611–622. doi:10.1016/j.jseaes.2014.08.019

Liu, J., Zhao, Y., Liu, X., Wang, Y., Wang, Y., and Liu, X. (2012). Rapid Exhumation of Basement Rocks Along the Northern Margin of the North China Craton in the Early Jurassic: Evidence from the Xiabancheng Basin, Yanshan Tectonic Belt. *Basin Res.* 24 (5), 544–558. doi:10.1111/j.1365-2117.2011.00538.x

Liu, S., Gurnis, M., Ma, P., and Zhang, B. (2017). Reconstruction of Northeast Asian Deformation Integrated with Western Pacific Plate Subduction since 200 Ma. *Earth-Science Rev.* 175 (1), 114–142. doi:10.1016/j.earscirev.2017.10.012

Liu, S., Li, Z., and Zhang, J. F. (2004). Mesozoic Basin Evolution and Tectonic Mechanism in Yanshan, China. *Sci. China Ser. D* 47, 24–38. doi:10.1360/04zd0022

Liu, S., Lin, C., Liu, X., and Zhuang, Q. (2018). Syn-tectonic Sedimentation and its Linkage to Fold-Thrusting in the Region of Zhangjiakou, North Hebei, China. *Sci. China Earth Sci.* 61 (6), 681–710. doi:10.1007/s11430-017-9175-3

Liu, S., Qian, T., Li, W., Dou, G., and Wu, P. (2015). Oblique Closure of the Northeastern Paleo-Tethys in Central China. *Tectonics* 34 (3), 413–434. doi:10.1002/2014tc003784

Liu, S., Steel, R., and Zhang, G. (2005). Mesozoic Sedimentary Basin Development and Tectonic Implication, Northern Yangtze Block, Eastern China: Record of Continent-Continent Collision. *J. Asian Earth Sci.* 25 (1), 9–27. doi:10.1016/j.jseaes.2004.01.010

Liu, S., Su, S., and Zhang, G. (2013). Early Mesozoic Basin Development in North China: Indications of Cratonic Deformation. *J. Asian Earth Sci.* 62, 221–236. doi:10.1016/j.jseaes.2012.09.011

Liu, S. (1998). The Coupling Mechanism of Basin and Orogen in the Western Ordos Basin and Adjacent Regions of China. *J. Asian Earth Sci.* 16 (4), 369–383. doi:10.1016/S0743-9547(98)00020-8

Liu, S. W., Lü, Y. J., Feng, Y. G., Liu, X. M., Yan, Q. R., Zhang, C., et al. (2007). Zircon and Monazite Geochronology of the Hongqiyingzi Complex, Northern Hebei, China. *Geol. Bull. China* 26, 1086–1100. (in Chinese).

Liu, S., and Yang, S. (2000). Upper Triassic - Jurassic Sequence Stratigraphy and its Structural Controls in the Western Ordos Basin, China. *Basin Res.* 12 (1), 1–18. doi:10.1046/j.1365-2117.2000.00107.x

Liu, S., Zhang, A., Lin, C., Zhang, B., Yuan, H., Huang, D., et al. (2021). Thrust Duplexing and Transpression in the Yanshan Mountains: Implications for Early Mesozoic Orogenesis and Decratonization of the North China Craton. *Basin Res.* 33, 2303–2327. doi:10.1111/bre.12558

Liu, S., Zhang, J., Hong, S., and Ritts, B. D. (2007). Early Mesozoic Basin Development and its Response to Thrusting in the Yanshan Fold-And-Thrust Belt, China. *Int. Geology Rev.* 49 (11), 1025–1049. doi:10.2747/0020-6814.49.11.1025

Liu, Y.-Q., Kuang, H.-W., Peng, N., Xu, H., Zhang, P., Wang, N.-S., et al. (2015). Mesozoic Basins and Associated Palaeogeographic Evolution in North China. *J. Palaeogeogr.* 4 (2), 189–202. doi:10.3724/SP.J.1261.2015.00073

Liu, Y., Gao, S., Hu, Z., Gao, C., Zong, K., and Wang, D. (2010). Continental and Oceanic Crust Recycling-Induced Melt-Peridotite Interactions in the Trans-North China Orogen: U-Pb Dating, Hf Isotopes and Trace Elements in Zircons from Mantle Xenoliths. *J. Pet.* 51 (1-2), 537–571. doi:10.1093/petrology/egp082

Liu, Y., Hu, Z., Gao, S., Günther, D., Xu, J., Gao, C., et al. (2008). In Situ analysis of Major and Trace Elements of Anhydrous Minerals by LA-ICP-MS without Applying an Internal Standard. *Chem. Geology* 257 (1–2), 34–43. doi:10.1016/j.chemgeo.2008.08.004

Ludwig, K. R. (2003). *User's Manual for Isoplot 3.00: A Geochronological Toolkit for Microsoft Excel*. Berkeley, CA: Berkeley Geochronology Center Special Publication, 1–74.

Ma, A., Hu, X., Garzanti, E., Han, Z., and Lai, W. (2017). Sedimentary and Tectonic Evolution of the Southern Qiangtang Basin: Implications for the Lhasa-Qiangtang Collision Timing. *J. Geophys. Res. Solid Earth* 122, 4790–4813. doi:10.1002/2017JB014211

Meng, Q.-R. (2003). What Drove Late Mesozoic Extension of the Northern China-Mongolia Tract? *Tectonophysics* 369 (3), 155–174. doi:10.1016/S0040-1951(03)00195-1

Meng, Q.-R., Wu, G.-L., Fan, L.-G., and Wei, H.-H. (2019). Tectonic Evolution of Early Mesozoic Sedimentary Basins in the North China Block. *Earth-Science Rev.* 190 (1), 416–438. doi:10.1016/j.earscirev.2018.12.003

Metelkin, D. V., Vernikovsky, V. A., Kazansky, A. Y., and Wingate, M. T. D. (2010). Late Mesozoic Tectonics of Central Asia Based on Paleomagnetic Evidence. *Gondwana Res.* 18 (2–3), 400–419. doi:10.1016/j.gr.2009.12.008

Nakapelukh, M., Bubniak, I., Yegorova, T., Murovskaya, A., Gintov, O., Shlapinskyi, V., et al. (2017). Balanced Geological Cross-Section of the Outer Ukrainian Carpathians Along the Pancake Profile. *J. Geodynamics* 108, 13–25. doi:10.1016/j.jog.2017.05.005

Niu, B. G., He, Z. J., Song, B., and Ren, J. S. (2003). SHRIMP Dating of the Zhangjiakou Formation Volcanics and its Geologic Significance. *Geol. Bull. China* 22, 140–141. (in Chinese).

Niu, Y., Liu, Y., Xue, Q., Shao, F., Chen, S., Duan, M., et al. (2015). Exotic Origin of the Chinese Continental Shelf: New Insights into the Tectonic Evolution of the Western Pacific and Eastern China Since the Mesozoic. *Sci. Bull.* 60 (18), 1598–1616. doi:10.1007/s11434-015-0891-z

Peng, P., Li, Y., Liu, F., and Wang, F. (2012). Geological Relation of Late Archean Lithologic Units in Northwest Hebei, North China Craton: Implication for Building of Early continental Crust. *Acta Petrologica Sinica* 28, 3531–3544. (in Chinese).

Peng, Y., Yu, S., Li, S., Liu, Y., Dai, L., Lv, P., et al. (2020). Early Jurassic and Late Cretaceous Granites in the Tongka Micro-block, Central Tibet: Implications for the Evolution of the Bangong-Nujiang Ocean. *J. Asian Earth Sci.* 194, 104030. doi:10.1016/j.jseaes.2019.104030

Qi, G.-w., Zhang, J.-J., and Wang, M. (2015). Mesozoic Tectonic Setting of Rift Basins in Eastern North China and Implications for Destruction of the North China Craton. *J. Asian Earth Sci.* 111, 414–427. doi:10.1016/j.jseaes.2015.06.022

Ren, J. Y., Tamaki, K., Li, S. T., and Zhang, J. X. (2002). Late Mesozoic and Cenozoic Rifting and its Dynamic Setting in Eastern China and Adjacent Areas. *Tectonophysics* 344 (3-4), 175–205. doi:10.1016/S0040-1951(01)00271-2

Riller, U., Clark, M. D., Daxberger, H., Doman, D., Lenauer, I., Plath, S., et al. (2017). Fault-slip Inversions: Their Importance in Terms of Strain, Heterogeneity, and Kinematics of Brittle Deformation. *J. Struct. Geology* 101, 80–95. doi:10.1016/j.jsg.2017.06.013

Shao, J. A., Meng, Q. R., Wei, H. Q., Zhang, L. Q., and Wang, P. Y. (2003). Nature and Tectonic Environment of the Late Jurassic Volcanic-Sedimentary Basins in Northwestern Heibei Province. *Geol. Bull. China* 22, 751–761. (in Chinese).

Shi, W., Dong, S.-W., Ratschbacher, L., Tian, M., Li, J.-H., and Wu, G.-L. (2013). Meso-Cenozoic Tectonic Evolution of the Dangyang Basin, north-central Yangtze Craton, central China. *Int. Geology Rev.* 55 (3), 382–396. doi:10.1080/00206814.2012.715732

Shi, W., Dong, S., and Hu, J. (2020). Neotectonics Around the Ordos Block, North China: A Review and New Insights. *Earth-Science Rev.* 200, 102969. doi:10.1016/j.earscirev.2019.102969

Shi, W., Dong, S., Zhang, Y., and Huang, S. (2015). The Typical Large-Scale Superposed Folds in the central South China: Implications for Mesozoic Intracontinental Deformation of the South China Block. *Tectonophysics* 664, 50–66. doi:10.1016/j.tecto.2015.08.039

Shi, W., Zhang, Y. Q., Ma, Y. S., Liu, G., and Wu, L. (2006). Formation and Modification History of the Liupanshan basin on the Southwestern Margin of the Ordos Block and Tectonic Stress Field Evolution. *Geology China* 33, 1066–1074. (in Chinese).

Shi, X., Liu, S., and Lin, C. (2019). Growth Structures and Growth Strata of the Qianjiadian Basin in the Western Yanshan Fold and Thrust Belt, North China. *Sci. China Earth Sci.* 62 (7), 1092–1109. doi:10.1007/s11430-018-9345-6

Song, H. L. (1985). Balanced Cross-Section and its Geological Significance. *Geol. Sci. Tech. Inf.* 4 (1), 18–28. (in Chinese).

Wallace, R. E. (1951). Geometry of Shearing Stress and Relation to Faulting. *J. Geology* 59, 118–130. doi:10.1086/625831

Wang, B.-D., Wang, L.-Q., Chung, S.-L., Chen, J.-L., Yin, F.-G., Liu, H., et al. (2016). Evolution of the Bangong-Nujiang Tethyan Ocean: Insights from the Geochronology and Geochemistry of Mafic Rocks within Ophiolites. *Lithos* 245, 18–33. doi:10.1016/j.lithos.2015.07.016

Wang, F., Chen, F., Siebel, W., Li, S.-Q., Peng, P., and Zhai, M.-G. (2011). Zircon U-Pb Geochronology and Hf Isotopic Composition of the Hongqiyingzi Complex, Northern Hebei Province: New Evidence for Paleoproterozoic and Late Paleozoic Evolution of the Northern Margin of the North China Craton. *Gondwana Res.* 20 (1), 122–136. doi:10.1016/j.gr.2011.02.003

Wang, G. C., Tan, Y. J., and Wang, F. Z. (1992). Multiphase Thrusting of the Chongli-Chicheng Regional Fracture of North Heibei Province and Tectonic Factors of Inner Mongolian Axis Upwarping. *Earth Science-Journal China Univ. Geosciences* 17 (6), 621–630. (in Chinese).

Wang, S. E., Gao, L. Z., Wan, X. Q., and Song, B. (2013). Ages of Tuchengzi Formation in Western Liaoning-Northern Hebei Area in Correlation with Those of International Strata. *Geol. Bull. China* 32, 1673–1690. (in Chinese).

Wang, T., Guo, L., Zhang, L., Yang, Q., Zhang, J., Tong, Y., et al. (2015). Timing and Evolution of Jurassic-Cretaceous Granitoid Magmatisms in the Mongol-Okhotsk belt and Adjacent Areas, NE Asia: Implications for Transition from Contractional Crustal Thickening to Extensional Thinning and Geodynamic Settings. *J. Asian Earth Sci.* 97, 365–392. doi:10.1016/j.jseaes.2014.10.005

Wang, T., Guo, L., Zheng, Y., Donskaya, T., Gladkochub, D., Zeng, L., et al. (2012). Timing and Processes of Late Mesozoic Mid-lower-crustal Extension in continental NE Asia and Implications for the Tectonic Setting of the Destruction of the North China Craton: Mainly Constrained by Zircon U-Pb Ages from Metamorphic Core Complexes. *Lithos* 154, 315–345. doi:10.1016/j.lithos.2012.07.020

Wang, T., Zheng, Y., Zhang, J., Zeng, L., Donskaya, T., Guo, L., et al. (2011). Pattern and Kinematic Polarity of Late Mesozoic Extension in Continental NE Asia: Perspectives from Metamorphic Core Complexes. *Tectonics* 30, TC6007. doi:10.1029/2011TC002896

Wang, Y., Dong, S., Chen, X., Shi, W., and Wei, L. (2018). Yanshanian Deformation Along the Northern Margin of the North China Craton: Constraints from Growth Strata in the Shiguai Basin, Inner Mongolia, China. *Basin Res.* 30 (6), 1155–1179. doi:10.1111/bre.12298

Wang, Y., Dong, S., Shi, W., Chen, X., and Jia, L. (2017). The Jurassic Structural Evolution of the Western Daqingshan Area, Eastern Yinshan Belt, North China. *Int. Geology. Rev.* 59 (15), 1885–1907. doi:10.1080/00206814.2017.1300784

Wang, Y., and Li, H. (2008). Initial Formation and Mesozoic Tectonic Exhumation of an Intracontinental Tectonic Belt of the Northern Part of the Taihang Mountain Belt, Eastern Asia. *J. Geology* 116 (2), 155–172. doi:10.1086/529153

Wang, Y., Sun, L., Zhou, L., and Xie, Y. (2018). Discussion on the Relationship Between the Yanshanian Movement and Cratonic Destruction in North China. *Sci. China Earth Sci.* 61, 499–514. doi:10.1007/s11430-017-9177-2

Wong, W. H. (1927). Crustal Movements and Igneous Activities in Eastern China since Mesozoic Time.1. *Bull. Geol. Soc. China* 6 (1), 9–37. doi:10.1111/j.1755-6724.1927.mp6001002.x

Wu, F.-Y., Sun, D.-Y., Ge, W.-C., Zhang, Y.-B., Grant, M. L., Wilde, S. A., et al. (2011). Geochronology of the Phanerozoic Granitoids in Northeastern China. *J. Asian Earth Sci.* 41 (1), 1–30. doi:10.1016/j.jseaes.2010.11.014

Wu, F., Lin, J., Wilde, S., Zhang, X., and Yang, J. (2005). Nature and Significance of the Early Cretaceous Giant Igneous Event in Eastern China. *Earth Planet. Sci. Lett.* 233 (1), 103–119. doi:10.1016/j.epsl.2005.02.019

Xiao, W., Windley, B. F., Hao, J., and Zhai, M. (2003). Accretion Leading to Collision and the Permian Solonker Suture, Inner Mongolia, China: Termination of the Central Asian Orogenic belt. *Tectonics* 22 (6), 1069. doi:10.1029/2002TC001484

Xu, H., Liu, Y.-Q., Kuang, H.-W., Jiang, X.-J., and Peng, N. (2012). U-pb SHRIMP Age for the Tuchengzi Formation, Northern China, and its Implications for Biotic Evolution During the Jurassic-Cretaceous Transition. *Palaeoworld* 21 (3-4), 222–234. doi:10.1016/j.palwor.2012.10.003

Xu, H., Liu, Y., Kuang, H., and Peng, N. (2016). Sedimentary Response to the Intracontinental Orogenic Process: Insight from the Anatomy of a Small Mesozoic Basin in Western Yanshan, Northern North China. *Int. Geology Rev.* 58 (12), 1528–1556. doi:10.1080/00206814.2016.1168323

Xu, H., Liu, Y., Kuang, H., and Peng, N. (2017). The 144-140 Ma Mafic Dykes in North China and Northeast China Indicating Regional Extensional Tectonic Setting. *Acta Geologica Sinica - English Edition* 91 (1), 353–354. doi:10.1111/1755-6724.13087

Xu, Y. G. (2004). Lithospheric Thinning Beneath North China: A Temporal and Spatial Perspective. *Geol. J. China Universities* 10, 324–331. (in Chinese).

Yang, Q. (2015). *Mesozoic Tectonic Deformation and Palaeostress Field Around Lamadong and Wangjiadian Areas in Jianchang County, Western Liaoning Province*. Beijing: China University of Geosciences, 1–70.

Yang, W., Li, S., and Jiang, B. (2007). New Evidence for Cretaceous Age of the Feathered Dinosaurs of Liaoning: Zircon U-Pb SHRIMP Dating of the Yixian Formation in Sihetun, Northeast China. *Cretaceous Res.* 28 (2), 177–182. doi:10.1016/j.cretres.2006.05.011

Yang, W. T., Wang, M., and Du, Y. S. (2014). The Depositional Characteristics from Mesozoic Jiyuan Basin with its Response to the Uplift of Qinling Orogen and Taihang Mountains. *Geol. Rev.* 60, 260–274. (in Chinese).

Yang, X., and Dong, Y. (2018). Mesozoic and Cenozoic Multiple Deformations in the Helanshan Tectonic Belt, Northern China. *Gondwana Res.* 60, 34–53. doi:10.1016/j.gr.2018.03.020

Yang, Y.-T. (2013). An Unrecognized Major Collision of the Okhotomorsk Block with East Asia During the Late Cretaceous, Constraints on the Plate Reorganization of the Northwest Pacific. *Earth-Science Rev.* 126 (1), 96–115. doi:10.1016/j.earscirev.2013.07.010

Zhai, M., Zhu, R., Liu, J., Meng, Q., Hou, Q., Hu, S., et al. (2004). Time Range of Mesozoic Tectonic Regime Inversion in Eastern North China Block. *Sci. China Ser. D-earth Sci.* 47 (2), 151–159. doi:10.1360/02yd0416

Zhang, B., Liu, S., Lin, C., Shen, W., and Li, X. (2020). Reconstruction of the Stress Regime in the Jiaolai Basin, East Asian Margin, as Decoded from Fault-Slip Analysis. *J. Struct. Geology* 141, 104190. doi:10.1016/j.jsg.2020.104190

Zhang, C. H. (1999). A Primary Discussion on the Intraplate Orogenic Belt. *Earth Sci. Front.* 6 (4), 295–308. (in Chinese).

Zhang, C. H., Li, C. M., Deng, H. L., Liu, Y., Liu, L., Wei, B., et al. (2011). Mesozoic Contraction Deformation in the Yanshan and Northern Taihang Mountains and its Implications to the Destruction of the North China Craton. *Sci. China: Earth Sci.* 54, 789–797. doi:10.1007/s11430-011-4203-410.1007/s11430-011-4180-7

Zhang, C. H., Zhang, Y., Li, H. L., Wu, Z. G., Wang, G. H., Xu, D. B., et al. (2006). Late Mesozoic Thrust Tectonics Framework in the Western Part in the Yanshan Orogenic Belt and the Western Hills of Beijing: Characteristics and Significance. *Earth Sci. Front.* 13, 165–183. (in Chinese).

Zhang, C., Wu, G., Wang, G., Zhang, W., and Song, H. (2004). Northwest Trending Tectonic belt in the Middle Yanshan Orogenic Belt of Northeast Hebei Province, North China: Tectonic Evolution and Geochronology. *Sci. China Ser. D-earth Sci.* 47, 896–911. doi:10.1360/03yd0073

Zhang, F. C. (2019).*Geochronology, Geochemistry and Geological Significance of the Xiaodaqingshan Granites in Jining, Inner Mongolia*. Beijing: China University of Geosciences, 1–59.

Zhang, G. W., Guo, A. L., Dong, Y. P., and Yao, A. P. (2019). Rethinking of the Qinling Orogen. *J. Geomechanics* 25 (5), 746–768. (in Chinese).

Zhang, H.-F., Zhai, M.-G., Santosh, M., Diwu, C.-R., and Li, S.-R. (2011). Geochronology and Petrogenesis of Neoarchean Potassic Meta-Granites from Huai'an Complex: Implications for the Evolution of the North China Craton. *Gondwana Res.* 20 (1), 82–105. doi:10.1016/j.gr.2011.01.009

Zhang, H., Wei, Z., Liu, X., and Li, D. (2009). Constraints on the Age of the Tuchengzi Formation by LA-ICP-MS Dating in Northern Hebei-Western Liaoning, China. *Sci. China Ser. D-earth Sci.* 52, 461–470. doi:10.1007/s11430-009-0052-9

Zhang, J., Wang, Y., Qu, J., Zhang, B., Zhao, H., Yun, L., et al. (2020). Mesozoic Intracontinental Deformation of the Alxa Block in the Middle Part of Central Asian Orogenic Belt: A Review. *Int. Geology Rev.* 1–31. doi:10.1080/00206814.2020.1783583

Zhang, P., Liu, Y. Q., Kuang, H. W., Peng, N., Xu, H., Liu, H., et al. (2014). Sedimentary Characteristics and Palaeogeography of the Mesozoic in Shangyi Basin, Northwestern Hebei Province. *J. Palaeogeogr.* 16, 359–376. doi:10.7605/gdlxb.2014.03.031

Zhang, Q., Wang, Y. L., Jin, W. J., and Li, C. D. (2008). Eastern China Plateau During the Late Mesozoic: Evidence, Problems and Implication. *Geol. Bull. China* 27, 1404–1430. (in Chinese).

Zhang, S.-H., Zhao, Y., Davis, G. A., Ye, H., and Wu, F. (2014). Temporal and Spatial Variations of Mesozoic Magmatism and Deformation in the North China Craton: Implications for Lithospheric Thinning and Decratonization. *Earth-Science Rev.* 131, 49–87. doi:10.1016/j.earscirev.2013.12.004

Zhang, Y. Q., and Dong, S. W. (2008). Mesozoic Tectonic Evolution History of the Tan-Lu Fault Zone, China: Advances and New Understanding. *Geol. Bull. China* 27, 1371–1139. (in Chinese).

Zhang, Y. Q., Dong, S. W., and Shi, W. (2003). Cretaceous Deformation History of the Middle Tan–Lu Fault Zone in Shandong Province, Eastern China. *Tectonophysics* 363 (3–4), 243–258. doi:10.1016/S0040-1951(03)00039-8

Zhang, Y. Q., Dong, S. W., Zhao, Y., and Zhang, T. (2007). Jurassic Tectonics of North China: A Synthetic View. *Acta Geologica Sinica* 81 (11), 1462–1480. (in Chinese).

Zhang, Y. Q., Zhao, Y., Dong, S. W., and Yang, N. (2004).Tectonic Evolution Stages of the Early Cretaceous Rift Basins in Eastern China and Adjacent Areas and Their Geodynamic Background. *Earth Sci. Front.*, 11, 123–133. (in Chinese).

Zhang, Y., Shi, W., Dong, S., Wang, T., and Yang, Q. (2020). Jurassic Intracontinental Deformation of the Central North China Plate: Insights from Syn-Tectonic Sedimentation, Structural Geology, and U Pb Geochronology of the Yungang Basin, North China. *Tectonophysics* 778, 228371. doi:10.1016/j.tecto.2020.228371

Zhao, G., Wilde, S. A., Sun, M., Guo, J., Kroner, A., Li, S., et al. (2008). SHRIMP U-Pb Zircon Geochronology of the Huai'an Complex: Constraints on Late Archean to Paleoproterozoic Magmatic and Metamorphic Events in the Trans-North China Orogen. *Am. J. Sci.* 308 (3), 270–303. doi:10.2475/03.2008.04

Zhao, Y. (1990). The Mesozoic Orogenies and Tectonic Evolution of the Yanshan Area. *Geol. Rev.* 36, 1–13. (in Chinese).

Zhao, Y., Zhang, S. H., Xu, G., Yang, Z. Y., and Hu, J. M. (2004). The Jurassic Major Tectonic Events of the Yanshanian Intraplate Deformation belt. *Geol. Bull. China* 23, 854–863. (in Chinese).

Zheng, T., Zhao, L., and Zhu, R. (2009). New Evidence from Seismic Imaging for Subduction during Assembly of the North China Craton. *Geology* 37 (5), 395–398. doi:10.1130/G25600A.1

Zheng, Y. D., Davis, G. A., Wang, C., Darby, B. J., and Zhang, C. H. (2000). Major Mesozoic Tectonic Events in the Yanshan belt and the Plate Tectonic Setting. *Acta Geologica Sinica* 74, 289–302. (in Chinese).

Zheng, Y., and Wang, T. (2005). Kinematics and Dynamics of the Mesozoic Orogeny and Late-Orogenic Extensional Collapse in the Sino-Mongolian Border Areas. *Sci. China Ser. D* 48, 849–862. doi:10.1360/03yd0552

Zhu, G., Chen, Y., Jiang, D., and Lin, S. (2015). Rapid Change from Compression to Extension in the North China Craton during the Early Cretaceous: Evidence from the Yunmengshan Metamorphic Core Complex. *Tectonophysics* 656, 91–110. doi:10.1016/j.tecto.2015.06.009

Zhu, G., Liu, C., Gu, C., Zhang, S., Li, Y., Su, N., et al. (2018). Oceanic Plate Subduction History in the Western Pacific Ocean: Constraint from Late Mesozoic Evolution of the Tan-Lu Fault Zone. *Sci. China Earth Sci.* 61, 386–405. doi:10.1007/s11430-017-9136-4

Zhu, R., Chen, L., Wu, F., and Liu, J. (2011). Timing, Scale and Mechanism of the Destruction of the North China Craton. *Sci. China Earth Sci.* 54 (6), 789–797. doi:10.1007/s11430-011-4203-4

Zhu, R., and Xu, Y. (2019). The Subduction of the West Pacific Plate and the Destruction of the North China Craton. *Sci. China Earth Sci.* 62 (9), 1340–1350. doi:10.1007/s11430-018-9356-y

Zhu, R., Xu, Y., Zhu, G., Zhang, H., Xia, Q., and Zheng, T. (2012). Destruction of the North China Craton. *Sci. China Earth Sci.* 55 (10), 1565–1587. doi:10.1007/s11430-012-4516-y

Zorin, Y. A. (1999). Geodynamics of the Western Part of the Mongolia-Okhotsk Collisional Belt, Trans-baikal Region (Russia) and Mongolia. *Tectonophysics* 306 (1), 33–56. doi:10.1016/S0040-1951(99)00042-6

Conflict of Interest: The authors declare that the research was conducted in the absence of any commercial or financial relationships that could be construed as a potential conflict of interest.

Publisher's Note: All claims expressed in this article are solely those of the authors and do not necessarily represent those of their affiliated organizations, or those of the publisher, the editors and the reviewers. Any product that may be evaluated in this article, or claim that may be made by its manufacturer, is not guaranteed or endorsed by the publisher.